

Precast Bent System for High Seismic Regions

Final Report, Appendix B: Design Example No. 1

Publication No. FHWA-HIF-13-037-B

June 2013

(Updated August 22, 2013)

HIGHWAYS FOR LIFE

Accelerating Innovation for the American Driving Experience.



Photo courtesy of the Precast/Prestressed Concrete Institute



U.S. Department of Transportation
Federal Highway Administration

Notice

This document is disseminated under the sponsorship of the U.S. Department of Transportation in the interest of information exchange. The U.S. Government assumes no liability for the use of the information contained in this document. This report does not constitute a standard, specification, or regulation.

The U.S. Government does not endorse products or manufacturers. Trademarks or manufacturers' names appear in this report only because they are considered essential to the objective of the document.

Quality Assurance Statement

The Federal Highway Administration (FHWA) provides high-quality information to serve Government, industry, and the public in a manner that promotes public understanding. Standards and policies are used to ensure and maximize the quality, objectivity, utility, and integrity of its information. FHWA periodically reviews quality issues and adjusts its programs and processes to ensure continuous quality improvement.

Technical Report Documentation Page

1. Report No. FHWA-HIF-13-037-B	2. Government Accession No. N/A	3. Recipient's Catalog No. N/A	
4. Title and Subtitle PRECAST BENT SYSTEM FOR HIGH SEISMIC REGIONS APPENDIX B: DESIGN EXAMPLE NO. 1		5. Report Date June 2013 (Updated August 22, 2013)	
		6. Performing Organization Code	
7. Author(s) M. Lee Marsh ¹ , Stuart J. Stringer ¹ , John F. Stanton ² , Marc O. Eberhard ² , Olafur S. Haraldsson ² , Hung Viet Tran ² , Bijan Khaleghi ³ , Eric Schultz ³ , and Steve Seguirant ⁴		8. Performing Organization Report No.	
9. Performing Organization Name and Address ¹ BergerABAM, Inc. 33301 Ninth Ave South, Suite 300 Federal Way, WA 98003 ² University of Washington, Seattle, WA ³ Washington State Department of Transportation, Olympia, WA ⁴ Concrete Technology Corporation, Tacoma, WA		10. Work Unit No.	
		11. Contract or Grant No. DTFH61-09-G-00005	
12. Sponsoring Agency Name and Address Federal Highway Administration Highways for LIFE Program Office 1200 New Jersey Avenue, SE Washington, DC 20590		13. Type of Report and Period Covered Final Report	
		14. Sponsoring Agency Code	
15. Supplementary Notes This is an appendix to the final project report, <i>Precast Bent System for High Seismic Regions</i> (FHWA-HIF-13-037).			
16. Abstract The final report for this project provides information on the system concept, as well as the background physical testing for the upper level grouted duct connections and the lower socket type connections. Additionally, the report provides design and construction specifications, describes a demonstration project constructed in Washington State, and discusses lessons learned from the demonstration project. This report is a technical resource that provides background information on the use of a precast bent system for use in high seismic regions. The system is designed for, and intended to be used with, prestressed girder bridges that are built integrally with the supporting intermediate piers. Appendix B documents the first of two design examples prepared to guide engineers through the application of the AASHTO Seismic Guide Specifications to the Highways for LIFE precast bridge bent system, along with the supplemental design provisions that have been proposed as an appendix to the Seismic Guide Specifications. Particular emphasis is given to the design and detailing of the connections between precast elements to ensure ductile energy dissipating behavior within the plastic hinge regions of the columns and capacity protection throughout the remainder of the structure. This design example uses an actual bridge recently designed by WSDOT, the US 12 Bridge over Interstate 5 at Grand Mound, which is also the demonstration project described in chapter 5 of the project report. There are two additional appendixes to the final report, published as stand-alone documents, as well as two companion reports that cover the detailed testing and modeling of the spread footing and drilled shaft foundation versions of the precast column-to-foundation connection: <ul style="list-style-type: none"> • Appendix A: Design Provisions (FHWA-HIF-13-037-A) • Appendix C: Design Example No. 2 (FHWA-HIF-13-037-C) • Laboratory Tests of Column-to-Drilled Shaft Socket Connections (FHWA-HIF-13-038) • Laboratory Tests of Column-to-Footing Socket Connections (FHWA-HIF-13-039) 			
17. Key Words Bridges, earthquakes, accelerated bridge construction, precast bent, connections, spread footing foundations, drilled shaft foundations, prefabricated bridge elements and systems		18. Distribution Statement No restrictions. This document is available to the public through the National Technical Information Service, Springfield, VA 22161.	
9. Security Classif. (of this report) Unclassified	20. Security Classif. (of this page) Unclassified	21. No. of Pages 99	22. Price

TABLE OF CONTENTS

CHAPTER 1. INTRODUCTION	1
Purpose.....	1
Applicable Specifications	1
Emphasis	1
Bridge Description	2
Bridge Length/Span	2
Curvature.....	2
Roadway Width	3
Pier Skew	3
Superstructure	3
Foundations.....	3
Connections.....	3
Materials	3
Response Spectrum.....	7
Site Classification	7
Seismic Hazard	7
Generation of the Design Response Spectra.....	9
CHAPTER 2. GENERAL DESIGN APPROACH	11
Design Procedure	11
Seismic Design Category.....	11
Earthquake Resisting System.....	12
Demand Analysis Procedure.....	12
Capacity Analysis Procedure	13
CHAPTER 3. ANALYSIS MODEL.....	15
General Overview	15
Superstructure	15
Cap Beams	15
Columns	16
Foundation Modeling.....	17
Spread Footings	17
Abutments	17
Material Modeling	17
CHAPTER 4. DEMAND ANALYSIS.....	19
Gravity Analysis	19
Modal Analysis	20
Response Spectrum Analysis.....	20
Demands	20
Verification of Modal Information	20
Response Spectrum Displacements	22

Displacement Magnification	22
Directional Uncertainty Combinations	24
Response Spectrum Forces	25
CHAPTER 5. CAPACITY ANALYSIS.....	27
Plastic Hinge Definitions	27
Plastic Hinge Lengths	27
Moment-Curvature Relationships	28
Axial Force-Moment Interaction Curves	31
Plastic Hinge Assignment	32
Capacities	33
Pushover Displacement Capacities	33
Inelastic Column Moment and Shear Demands.....	34
CHAPTER 6. DESIGN CHECKS.....	37
Displacement Capacity-to-Demand Ratio	37
Member Ductility	37
Longitudinal Direction.....	38
Transverse Direction.....	39
Column Plastic Hinge Shear Capacity-to-Demand Ratio.....	40
Longitudinal Direction.....	42
Transverse Direction.....	43
P- Δ Effects	44
Support Length.....	45
Capacity-Protected Member Capacities.....	46
Superstructure	46
Shear Blocks	46
Prestressed Girder Anchorage.....	47
Cap Beam.....	49
Column-to-Cap Beam Connection.....	51
Column Splices	67
Spread Footing	72
Socket Connection of Column to Spread Footing	74
CHAPTER 7. CONSTRUCTABILITY CONSIDERATIONS	77
Size of Precast Elements.....	77
Transportation Dimension and Weight Restrictions.....	77
Crane Pick Weight	77
Transportation and Erection Loading	77
Cap Beam Fit-up with Columns	77
Construction Sequence.....	78
CHAPTER 8. CLOSING REMARKS	81
ACKNOWLEDGEMENTS	83

REFERENCES.....85

LIST OF FIGURES

Figure 1. Diagram. Bridge plan and elevation.....	4
Figure 2. Diagram. Typical precast pier and cast-in-place footing.....	5
Figure 3. Diagram. Intermediate pier cap beam plan and elevation.	6
Figure 4. Screen shot. USGS/AASHTO ground motion tool window used to determine design parameters and response spectra.	7
Figure 5. Screen shot. USGS/AASHTO ground motion tool window presenting site coefficients.	8
Figure 6. Graph. Design response spectrum.	9
Figure 7. Equation. Calculating S_a for periods greater than T_s	9
Figure 8. Diagram. Isometric view of bridge spine model.	15
Figure 9. Graph. Effective flexural stiffness of rectangular cracked reinforced concrete sections (figure 5.6.2-1 in the Seismic Guide Specifications).	19
Figure 10. Equation. Base shear.	21
Figure 11. Equation. Short period amplification factor.	23
Figure 12. Equation. Short period acceleration.	23
Figure 13. Equation. Analytical plastic hinge length.....	27
Figure 14. Graph. Column length definitions.	28
Figure 15. Graph. Column concrete stress-strain relationships.	29
Figure 16. Graph. ASTM A706 reinforcement stress-strain relationship.....	30
Figure 17. Graph. Typical moment-curvature relationship (axial load = 1,000 kips).	31
Figure 18. Diagram. Column P-M interaction curve.	32
Figure 19. Graph. Longitudinal direction pushover curve.....	33
Figure 20. Graph. Transverse direction pushover curve.	34
Figure 21. Equation. Displacement capacity-to-demand ratio requirement.	37
Figure 22. Equation. Displacement ductility demand.....	37
Figure 23. Equation. Idealized yield displacement.	38
Figure 24. Equation. Plastic displacement demand.	38
Figure 25. Equation. Plastic curvature demand.	38
Figure 26. Equation. Shear capacity requirement.	41
Figure 27. Equation. Concrete shear resistance.	41
Figure 28. Equation. Effective area.	41

Figure 29. Equation. Concrete shear resistance if the column is in compression.....	41
Figure 30. Equation. Concrete shear stress adjustment factor.	41
Figure 31. Equation. Calculating f_s	41
Figure 32. Equation. Volumetric ratio of transverse steel.	41
Figure 33. Equation. Concrete shear resistance if the column is in tension.	42
Figure 34. Equation. Steel shear resistance.	42
Figure 35. Equation. P- Δ check.	44
Figure 36. Equation. Number of extended strands.	47
Figure 38. Diagram. Extended strand design (from WSDOT BDM). ⁽³⁾	48
Figure 39. Diagram. Longitudinal force transfer at the cap beam interface.	52
Figure 40. Diagram. Longitudinal effective superstructure width.....	52
Figure 41. Equation. Column longitudinal bar anchorage length.....	53
Figure 42. Equation. Available axial bar stress.	53
Figure 43. Diagram. Interface mechanics.	54
Figure 44. Equation. Tensile resultant force.....	54
Figure 45. Diagram. Interface geometry.....	55
Figure 46. Equation. Distance to the tensile force resultant.	56
Figure 47. Graph. Interface moment-curvature response.	57
Figure 48. Graph. Interface net tensile force.	57
Figure 49. Diagram. Transverse loading—horizontal normal joint stress.....	58
Figure 50. Diagram. Transverse loading—vertical joint shear stress.	58
Figure 51. Diagram. Transverse loading—vertical normal joint stress.....	59
Figure 52. Diagram. Longitudinal loading—horizontal normal joint stress.....	59
Figure 53. Diagram. Longitudinal loading—vertical joint shear stress.....	60
Figure 54. Diagram. Longitudinal loading—vertical normal joint stress.....	60
Figure 55. Equation. Column tensile force associated with plastic hinging.....	61
Figure 56. Equation. Vertical joint shear stress from loading in the transverse direction.	61
Figure 57. Equation. Minimum vertical joint shear stress from loading in the transverse direction.	61
Figure 58. Equation. Maximum vertical joint shear stress from loading in the transverse direction.	61
Figure 59. Equation. Horizontal normal joint stress from loading in the transverse direction.....	62
Figure 60. Equation. Principal tension from loading in the transverse direction.	62

Figure 61. Equation. Principal compression from loading in the transverse direction.....	62
Figure 62. Equation. Ultimate principal compression.	62
Figure 63. Equation. Ultimate principal tension.....	63
Figure 64. Equation. Cracking principal tension.	63
Figure 65. Equation. Minimum volumetric reinforcing ratio for cracked joints.	63
Figure 66. Equation. Spacing of transverse reinforcement.....	63
Figure 67. Equation. Area of joint vertical reinforcement.....	64
Figure 68. Equation. Area of joint horizontal reinforcement.....	64
Figure 69. Equation. Area of joint side reinforcement.	64
Figure 70. Equation. Area of J-bar reinforcement.	64
Figure 71. Equation. Vertical joint shear stress from loading in the longitudinal direction.....	65
Figure 72. Equation. Minimum vertical joint shear stress from loading in the longitudinal direction.	65
Figure 73. Equation. Maximum vertical joint shear stress from loading in the longitudinal direction.	65
Figure 74. Equation. Horizontal normal joint stress from loading in the longitudinal direction..	66
Figure 75. Equation. Principal tension from loading in the longitudinal direction.	66
Figure 76. Equation. Principal compression from loading in the longitudinal direction.....	66
Figure 77. Equation. Ultimate principal compression.	66
Figure 78. Equation. Ultimate principal tension.....	66
Figure 79. Equation. Cracking principal tension.	67
Figure 80. Equation. Minimum volumetric reinforcing ratio for uncracked joints.	67
Figure 81. Equation. Spacing of transverse reinforcement.....	67
Figure 82. Diagram. Top of column segment.	68
Figure 83. Diagram. Middle column segment.	69
Figure 84. Diagram. Bottom of column segment.	69
Figure 85. Equation. Nominal shear friction capacity.	70
Figure 86. Equation. First upper limit of shear friction capacity.....	70
Figure 87. Equation. Second upper limit of shear friction capacity.	70
Figure 88. Equation. Development length for a bar grouted into a metal duct.....	70
Figure 89. Diagram. Flexural demands on column splices.....	71
Figure 90. Equation. Base development length.	71
Figure 91. Diagram. Adjustment of footing flexural reinforcement.....	73

Figure 92. Diagram. Precast column strut-and-tie mechanism.....	74
Figure 93. Diagram. Conventional cast-in-place column strut-and-tie mechanism.	74
Figure 94. Diagram. Additional shear friction reinforcement.	75
Figure 95. Equation. Nominal shear friction capacity.	75
Figure 96. Equation. Capacity of column-to-footing interface.....	75
Figure 97. Equation. Minimum required shear friction reinforcement.....	76
Figure 98. Diagram. Footing reinforcement plan.	76
Figure 99. Photos. Construction sequence for placement of first precast column segment.	79
Figure 100. Photo. Precast cap beam placement.....	79

LIST OF TABLES

Table 1. Design example matrix.	1
Table 2. Foundation spring properties.	17
Table 3. Material properties.	17
Table 4. Model verification: total weight.	21
Table 5. Model verification: base shear transverse direction.	21
Table 6. Top of column displacements—global coordinates.	22
Table 7. Top of column displacements—local coordinates.	22
Table 8. Top of column magnified displacements.	23
Table 9. Top of column magnified displacements.	24
Table 10. ASTM A706, Grade 60 properties.	30
Table 11. Curvature limits.	31
Table 12. Pier displacement capacities.	34
Table 13. In-plane pier design forces.	35
Table 14. Out-of-plane pier design forces.	35
Table 15. Displacement capacity-to-demand check.	37
Table 16. Ductility demands, longitudinal direction—top hinge.	39
Table 17. Ductility demands, longitudinal direction—bottom hinge.	39
Table 18. Ductility demands, transverse direction—top hinge.	40
Table 19. Ductility demands, transverse direction—bottom hinge.	40
Table 20. Longitudinal hinge shear C/D check.	43
Table 21. Transverse hinge shear C/D check.	44
Table 22. P- Δ check—transverse.	45
Table 23. P- Δ check—longitudinal.	45
Table 24. Interface geometry.	55

LIST OF ABBREVIATIONS AND ACRONYMS

AASHTO	American Association of State Highway and Transportation Officials
ABC	Accelerated bridge construction
DC	Dead load of structural components and nonstructural attachments
DW	Dead load of wearing surfaces and utilities
FHWA	Federal Highway Administration
HfL	Highways for LIFE
P-M	Axial load-moment
SDC	Seismic Design Category
WSDOT	Washington State Department of Transportation

CHAPTER 1. INTRODUCTION

PURPOSE

This is the first of a set of two seismic design examples created for this project. A different bridge is used in each design example. The goal of the design examples is to cover the features that must be addressed in the seismic design process for a fully precast bridge system. Table 1 is a matrix of the features in this seismic design example.

Table 1. Design example matrix.

Description	Two-span continuous
Plan Geometry	Tangent, skew
Superstructure Type	Prestressed precast concrete girder
Pier Type	Precast four-column, spliced, dropped cap bent
Abutment Type	Tall abutment with overhanging end diaphragm
Foundation Type	Spread footing, Site Class C
Connections and Joints	Socket connection to footing, integral at intermediate pier, elastomeric bearing pads (abutments)

APPLICABLE SPECIFICATIONS

The design examples conform to the following specifications:

- American Association of State Highway and Transportation Officials (AASHTO) Guide Specifications for LRFD [Load and Resistance Factor Design] Seismic Bridge Design, Second Edition (herein called “Seismic Guide Specifications”).⁽¹⁾
- AASHTO LRFD Bridge Design Specifications, Fifth Edition (herein called “Bridge Design Specifications”).⁽²⁾
- Washington State Department of Transportation, Bridge Design Manual, M23-50.04, 2010 (herein called “WSDOT BDM”).⁽³⁾

Additionally, the design of the precast column and its connections to the foundation and cap beam and the seismic design of the cap beam are supplemented by draft design specifications contained in appendix A of this report, in addition to the University of Washington research reports supporting this Highways for LIFE project.^(4,5)

EMPHASIS

This design example follows the design procedures of the Seismic Guide Specifications. The emphasis of this example is to focus on the demand analysis and capacity design checks required by the Seismic Guide Specifications, specifically applied to a fully precast integral bent system for high seismic areas. Below is a list of the design considerations that will be addressed:

- General seismic design and analysis philosophy in the Seismic Guide Specifications and how they apply to the Highways for LIFE bent system.

- Structural seismic demand analysis using an elastic centerline bridge model, a multimodal response spectrum analysis, and the coefficient method of predicting the nonlinear displacement demands.
- Structural capacity analysis (i.e., pushover analysis) including the development of nonlinear moment-curvature and axial load-moment (P-M) interaction relationships, plastic hinge definition, and the displacement capacity of the system.
- Plastic design forces.
- Displacement capacity to demand ratios.
- Individual member ductility demands.
- Column plastic hinge shear capacity to demand ratios.
- P- Δ Effects.
- Required support lengths at the abutments.
- Capacity protection of the following members or components:
 - Superstructure (precast prestressed concrete girders).
 - Prestressed concrete girder strand development at the intermediate pier to provide continuity of the girders.
 - Shear blocks at the abutments to resist transverse design forces.
 - Precast cap beam for seismic as well as construction, transportation, and erection loading.
 - Column-to-cap beam connection and joint design with an emphasis on the special considerations particular to an integral dropped cap beam.
 - The splice between column segments.
 - The column to a cast-in-place spread footing socket connection.
- Constructability considerations such as shipment and crane pick weight restrictions, fit-up between precast elements, tolerances, and construction sequence.

BRIDGE DESCRIPTION

The bridge used in this design example is the Grand Mound to Maytown bridge replacement north of the city of Centralia on Interstate 5 in Washington State. The structural details are described below and shown in figures 1 through 3.

Bridge Length/Span

The bridge has two spans and is 176 feet long from back to back of pavement seats at the abutments. The spans are symmetrical at 88 feet each.

Curvature

The bridge is straight. No horizontal curvature exists.

Roadway Width

The roadway is 71 feet wide, measured from curb line to curb line.

Pier Skew

All piers are uniformly oriented at an angle of 29.19 degrees from a line perpendicular to the bridge centerline.

Superstructure

The superstructure is made up of thirty 2-foot 11-5/8-inch deep prestressed precast deck-bulb tee girders spaced at 5 feet 9 inches on center (WSDOT Series W35DG). The girders are made integral with the substructure using a full depth cast-in-place diaphragm. The girders include a precast end diaphragm at the intermediate pier to reduce the need for stage two cap beam formwork. The roadway is a 5-inch-thick cast-in-place topping slab with a total width of 84 feet.

Substructure

The substructure consists of an abutment at each end and a precast concrete intermediate pier, which is made up of a 3-foot-deep by 6-foot 6-inch-wide dropped precast concrete cap beam supported by four square precast concrete columns. The full cap beam consists of a precast lower stage that has been made integral with the full depth cast-in-place diaphragm above. The columns are 4 feet wide for the bottom 6 feet, and then taper at 1:48 up to the cap beam. The square section is terminated 3 inches from the footing and the cap beam connections, and is replaced with a 4-foot-diameter circular section.

The column height for all columns at the intermediate pier location ranges from 19 feet 2 inches to 20 feet 10 inches, measured from the top of the footing to the soffit of the dropped cap beam.

Foundations

Each column at the intermediate pier is supported by a cast-in-place spread footing 18 feet by 18 feet by 4 feet 9 inches deep.

Connections

The ends of the precast girders are integrally connected to the diaphragm at the intermediate pier. The abutments provide full restraint in the direction transverse to the bridge centerline and no restraint in the direction parallel to the bridge centerline.

Materials

The concrete has a nominal compressive strength of 4,000 psi for precast and cast-in-place elements. Steel reinforcement is A706 Grade 60.

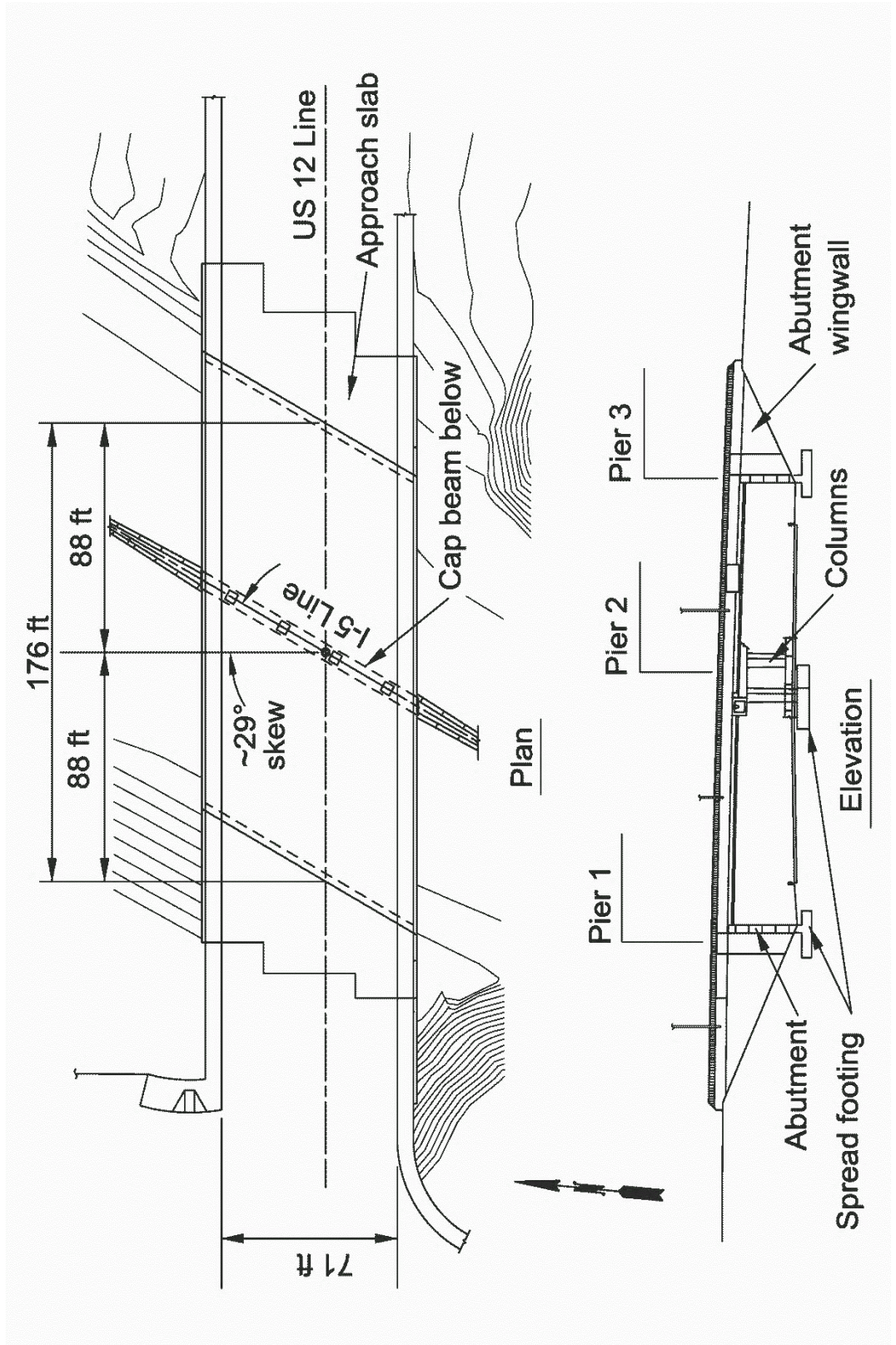


Figure 1. Diagram. Bridge plan and elevation.

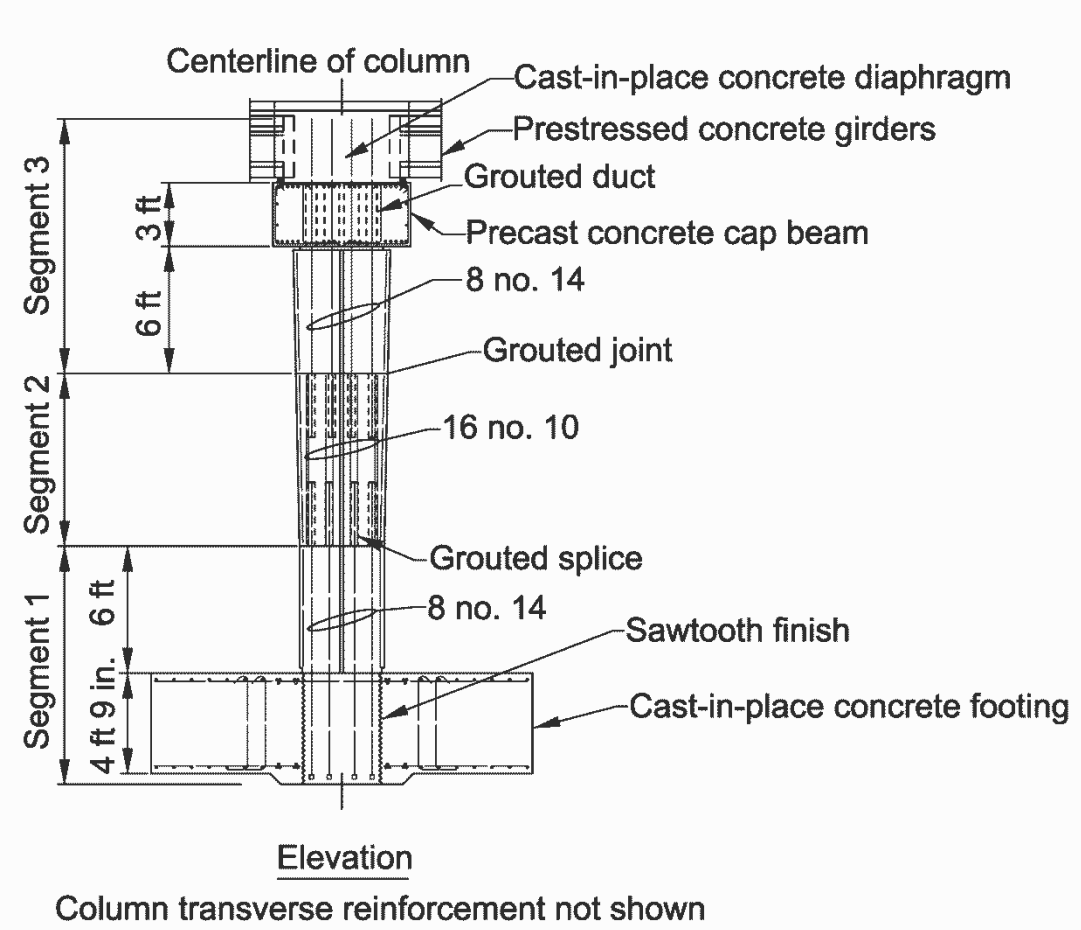


Figure 2. Diagram. Typical precast pier and cast-in-place footing.

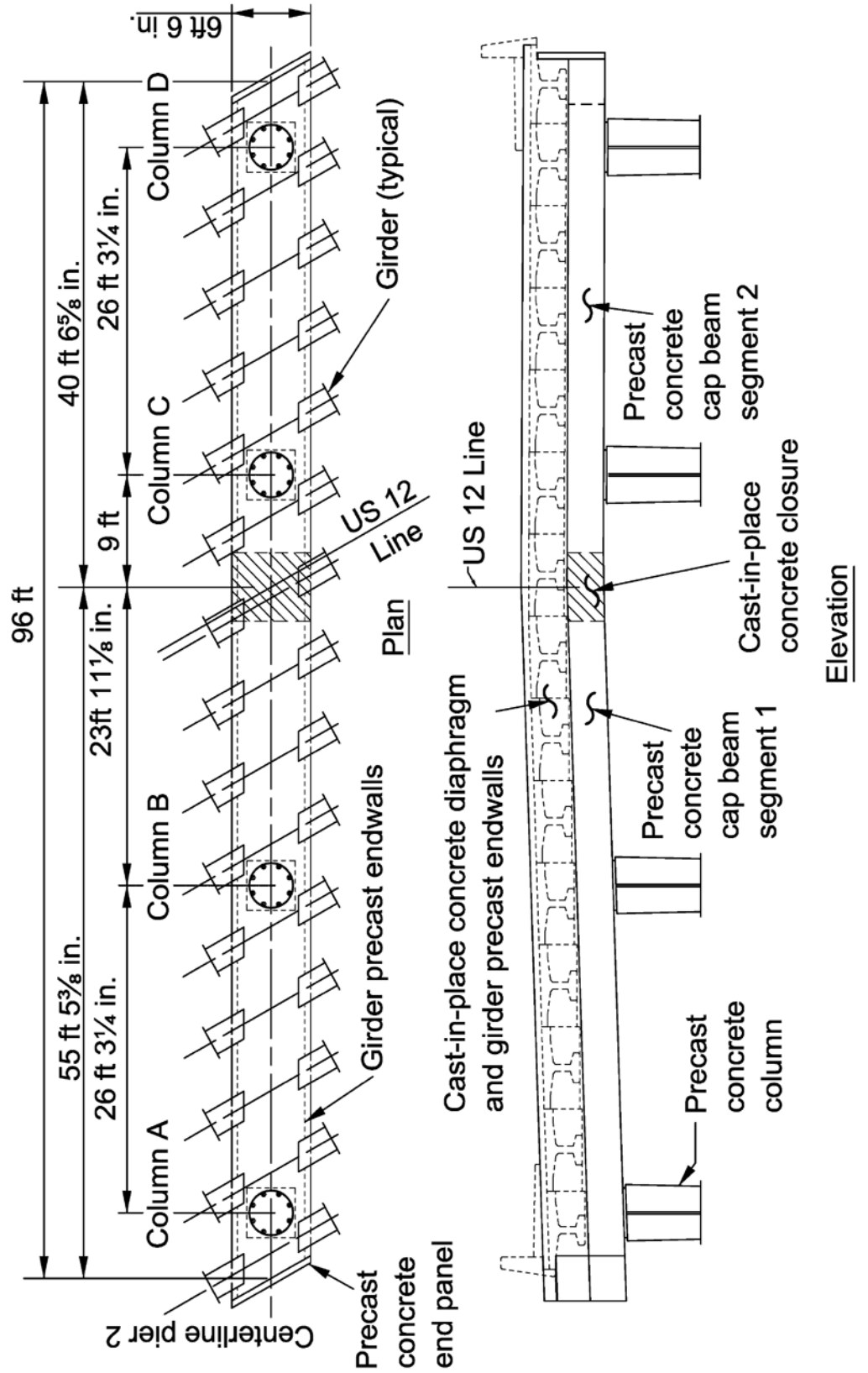


Figure 3. Diagram. Intermediate pier cap beam plan and elevation.

RESPONSE SPECTRUM

Site Classification

The bridge is located in a site that is classified as Site Class C. The various site classifications are defined in article 3.4.2.1 of the Seismic Guide Specifications. Typically, the site classification is defined by the geotechnical engineer.

Seismic Hazard

The seismic ground shaking hazard is characterized using an acceleration response spectrum. The Seismic Guide Specifications allow for the use of either a general acceleration response spectrum or a site-specific acceleration response spectrum provided by a geotechnical engineer. In this example, the general acceleration response spectrum is used. The bridge is located near Grand Mound, Washington (zip code 98579), at the following latitude and longitude:

- Latitude: 46.8024.
- Longitude: -123.0072.

The United States Geological Survey (USGS) developed a ground motion tool that runs from a CD-ROM that accompanies the Seismic Guide Specifications, or the tool can be found on the USGS website under a heading for AASHTO. The program was used to determine the design parameters. Figures 4 and 5 show the typical windows from the USGS/AASHTO seismic design parameters CD-ROM. Input can be either latitude and longitude or zip code.

The screenshot displays a software interface for calculating seismic design parameters. It is divided into two main panels: 'Input Data and Parameter Calculations' on the left and 'Output Calculations and Ground Motion Maps' on the right.

Input Data and Parameter Calculations:

- Select Geographic Region:** A dropdown menu is set to 'Conterminous 48 States'.
- Guidelines Edition:** A text box contains '2007 AASHTO Bridge Design Guidelines'.
- Specify Site Location by Latitude-Longitude or Zip Code:** Radio buttons are set to 'Latitude-Longitude : Recommended'. Input fields show '46.802476' for Latitude (range 50.0 to 24.6) and '-123.007237' for Longitude (range -125.0 to -65.0).
- Calculate Basic Design Parameters:** A dropdown for 'Probability of Exceedance' is set to '7% PE in 75 years'. Two buttons are present: 'Calculate PGA, Ss, and S1' and 'Calculate As, SDs, and SD1'.
- Calculate Response Spectra:** Three buttons are present: 'Map Spectrum', 'Design Spectrum', and 'View Spectra'.

Output Calculations and Ground Motion Maps:

The output panel displays the following information:

- Conterminous 48 States
- 2007 AASHTO Bridge Design Guidelines
- AASHTO Spectrum for 7% PE in 75 years
- Latitude = 46.802476
- Longitude = -123.007237
- Site Class B
- Data are based on a 0.05 deg grid spacing.

Period (sec)	Sa (g)	PGA - Site Class B
0.0	0.347	PGA - Site Class B
0.2	0.772	Ss - Site Class B
1.0	0.301	S1 - Site Class B

At the bottom of the output panel, there are two buttons: 'Clear Output' and 'View Maps'.

Figure 4. Screen shot. USGS/AASHTO ground motion tool window used to determine design parameters and response spectra.

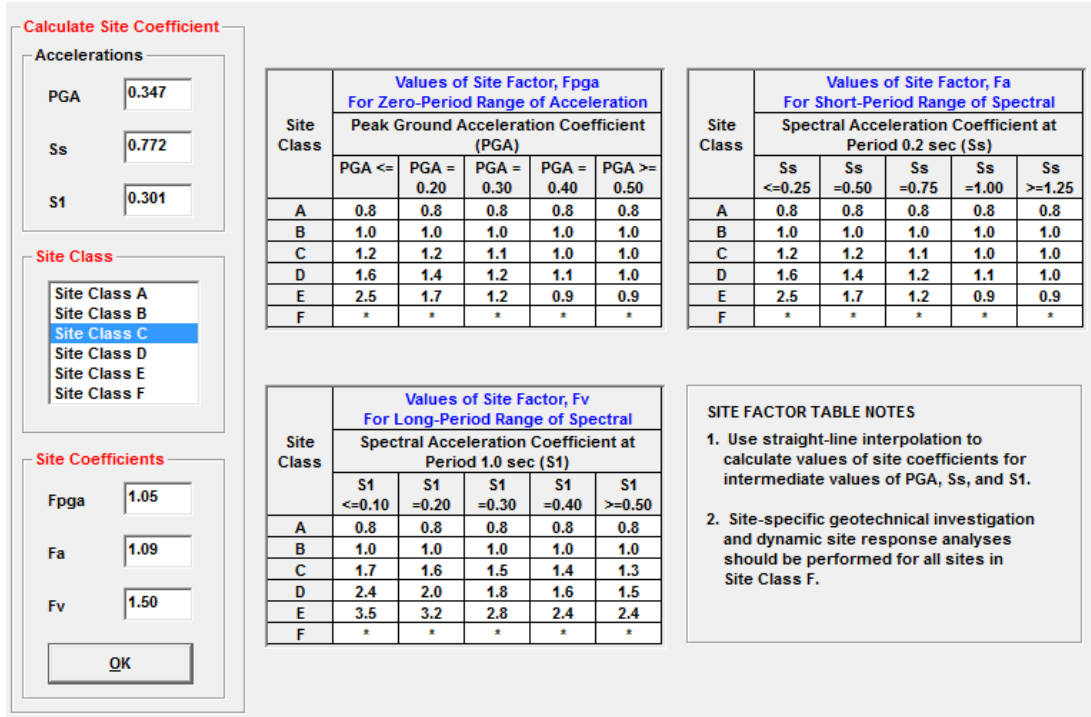


Figure 5. Screen shot. USGS/AASHTO ground motion tool window presenting site coefficients.

The seismic hazard is characterized using the response corresponding to a rock site (Site Class B), and then the effects of the local site soil are introduced with adjustment coefficients. The rock motions are characterized using Site Class B, and then these are modified depending on the site class.

From the USGS/AASHTO seismic hazard maps, the mapped spectral acceleration coefficients for Site Class C are as follows:

$$PGA = 0.347 \text{ g}$$

$$S_s = 0.772 \text{ g}$$

$$S_1 = 0.301 \text{ g}$$

The site coefficients are:

$$F_{PGA} = 1.05$$

$$F_a = 1.09$$

$$F_v = 1.50$$

The general acceleration response spectrum is generated from the following parameters:

$$A_s = (PGA)(F_{PGA}) = 0.364 \text{ g}$$

$$S_{DS} = (F_a)(S_s) = 0.842 \text{ g}$$

$$S_{D1} = (F_v)(S_1) = 0.451 \text{ g}$$

Where:

A_s = Acceleration coefficient

S_{DS} = Short period acceleration coefficient

S_{D1} = 1-second period acceleration coefficient

Generation of the Design Response Spectra

The general horizontal acceleration design response spectrum was generated following the three-point construction method of article 3.4.1 of the Seismic Guide Specifications and is shown in figure 6.

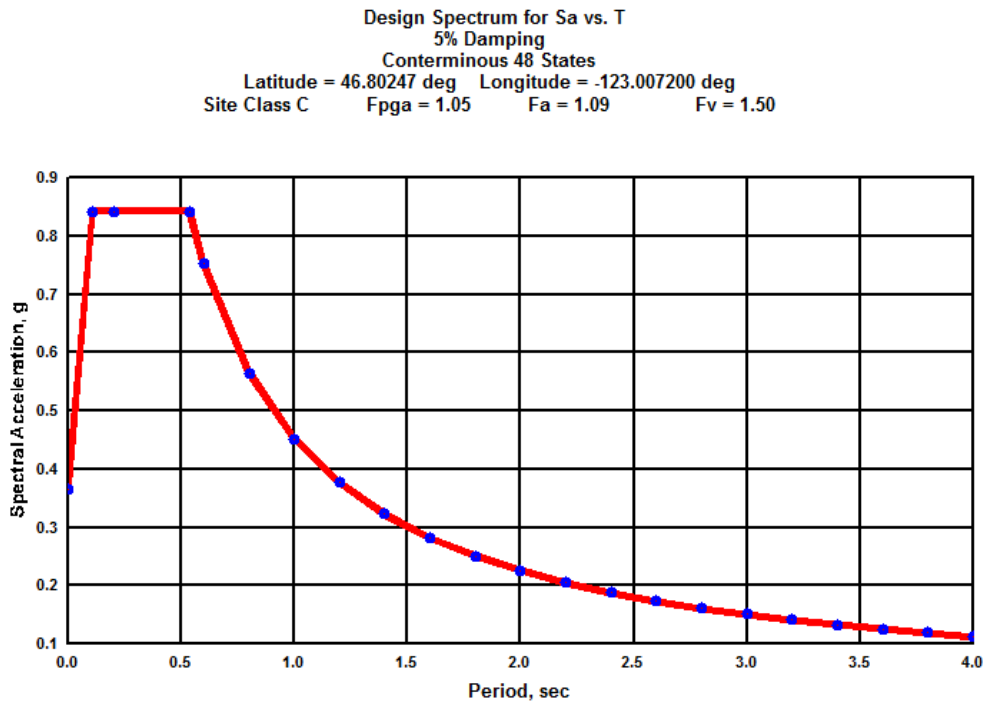


Figure 6. Graph. Design response spectrum.

The general design acceleration response spectrum is specified as a function of period. The general design curve was developed as follows:

- **Periods less than T_o .** The design response spectrum acceleration, S_a , increases linearly from A_s to S_{DS} .
- **Periods between T_o and T_s .** The curve is capped. S_a equals S_{DS} .
- **Periods greater than T_s .** S_a decreases proportionately to the inverse of the period. In equation format, this is defined as shown in figure 7.

$$S_a = S_{D1}/T = 0.451g/T$$

Figure 7. Equation. Calculating S_a for periods greater than T_s .

CHAPTER 2. GENERAL DESIGN APPROACH

The Seismic Guide Specifications apply to the design of conventional bridges, and not to the design of bridges considered “essential” or “critical.” For essential bridges, and for bridge construction types not covered by the Seismic Guide Specifications, project-specific criteria should be developed. Conventional bridges shall be designed for a “life safety” performance objective based on a seismic hazard corresponding to a 7 percent probability of exceedance in 75 years. Life safety shall be understood to mean that the bridge has a low probability of collapse, but significant damage and disruption of traffic may occur. The bridge may need to be replaced after the design seismic event.

DESIGN PROCEDURE

The design procedure should start with understanding the seismic hazard, the site conditions, and the Seismic Design Category (SDC). The seismic hazard and site conditions were defined in the introduction to this example. An extended determination of the SDC is shown in the next subsection.

Based on the SDC, the earthquake resisting system (ERS) must be identified. For SDCs C and D, the Seismic Guide Specifications require the ERS to be clearly identifiable to achieve the life safety requirements. For SDC B, the ERS shall be considered. The ERS must provide a reliable and direct load path for transferring the seismically induced forces into the soil and provide sufficient means of energy dissipation and/or restraint to adequately control seismic-induced displacements. All structural elements must be capable of achieving the anticipated displacements for the design strategy chosen. The Seismic Guide Specifications identify three different design strategies:

- **Type I:** Design a ductile substructure with an essentially elastic superstructure.
- **Type II:** Design an essentially elastic substructure with a ductile superstructure.
- **Type III:** Design an elastic superstructure and substructure with a fusing mechanism at the interface between the superstructure and the substructure.

Permissible ERS and earthquake resisting elements (EREs) are defined in article 3.3 of the Seismic Guide Specifications. For an ERS to be permissible, all EREs incorporated in the design must also be permissible. If not, the ERS must be considered “not recommended for new construction” unless approved by the owner. There is an intermediate category of EREs that are permissible, but only with the approval of the owner. The intent of this category is to permit certain construction details that are not optimum for seismic resistance but are acceptable with the owner’s approval. EREs in this category often involve seismic damage locations that are difficult to inspect and repair.

Seismic Design Category

The SDC, defined in article 3.5 of the Seismic Guide Specifications, is based on the 1-second period design spectral acceleration, S_{DI} . The SDC determines the analysis and design

requirements for the particular bridge site. In this design example, S_{DI} was calculated to be 0.451 g, which places the bridge in SDC C. The required design checks of SDC C include:

- Identification of ERS.
- Demand analysis.
- Implicit capacity check required (displacement, P- Δ , and support length).
- Capacity design required, including column shear requirement.
- SDC C level of detailing.
- Liquefaction evaluation required (not covered in this design example).

Earthquake Resisting System

The bridge in this design example is located in SDC C and, thus, an ERS must be defined. The bridge will be designed as a Type I structure. Damage or yielding will be localized to the top and bottom of the columns (i.e., in selected plastic hinge zones). Thus, the columns will be the EREs. The superstructure and foundation components will be designed to remain elastic. In the longitudinal direction, the abutments will provide passive resistance from the soil backfill, but no resistance was assumed for the design. This conservatively puts the longitudinal force on the intermediate pier. In the transverse seismic event, the abutments will provide lateral restraint and should be designed for appropriate forces.

Demand Analysis Procedure

The seismic demand analysis of the bridge is a multi-phase process. The first phase involves generating the demand analysis models. Development of the analysis model includes calculation of member properties, geometry, boundary conditions, foundation stiffnesses, seismic mass/weight, input acceleration spectrum, and internal releases. The column plastic hinge interaction surfaces and curvature limitations need to be defined and entered into the analysis model or need to be considered by hand analysis. A gravity dead load check should be made by hand calculations against the seismic model output. The model should also be checked to ensure that the model has adequate mass participation (at least 90 percent mass participation in both the transverse and longitudinal directions) and produces the anticipated directional base shear based on the period of the structure in the direction under consideration.

The next phase involves running the demand model that typically consists of multimodal linear elastic response spectrum analyses. These analyses are used to define the displacement demands used to assess the ductile structural elements. This phase of analysis also serves to define the elastic demands on the capacity-protected structural elements. The plastic overstrength capacity of the ductile elements (i.e., plastic hinging forces in the columns) will become the plastic overstrength demands on the capacity-protected elements. The minimum of the elastic and plastic overstrength demands will define the seismic demands on the capacity-protected elements. Capacity protecting non-ductile elements decouples their response from the design earthquake and ensures that the seismic fuses remain where they were intended by the designer to be.

Notes to Designers

The demand analysis procedure appears linear. However, because the Seismic Guide Specifications utilize displacement demand rather than force as a basis for acceptability, the process should be expected to be iterative to come up with an efficient/economical design. As the Seismic Guide Specifications are used to check displacement criteria, the designer should keep in mind that force-based criteria are still in effect from other load combinations in the Bridge Design Specifications. For example, wind and temperature cases should be run prior to any seismic analysis to determine minimum anticipated column size and reinforcing. Unlike force-based designs, in the Seismic Guide Specifications determination of the column section is an iterative process. In this example, column section requirements from non-seismic analyses were taken to be less than the minimums required by the Seismic Guide Specifications.

For this design, columns of various diameters were checked as potential candidates for the intermediate pier. For each column size, different percentages of longitudinal steel and transverse confinement were also investigated. Variation of these parameters affects the behavior of the column under applied loads. Axial force-moment interaction relationships (P-M curves) must be accounted for. Additionally, moment-curvature ($M-\phi$) relationships are dependent on the column reinforcement, material strengths, and axial load. This relationship is vitally important to displacement based design. A useful tip to the designer would be to create a table of different plastic hinge configurations based on different longitudinal and transverse reinforcement ratios for use in multiple projects before running the capacity analyses so that the hinges can be easily swapped out and compared during the analysis stage. It should be noted that changing the diameter of the column at the analysis stage will require a return to the elastic demand model, as the stiffness of the column will change due to the section geometry. Also note that larger confining steel typically results in larger overall displacement capacities, while increasing longitudinal steel typically increases moment capacity.

Capacity Analysis Procedure

After the demand analyses are completed, the capacity analyses should be run. The bridge in this design example is located in SDC C, which requires implicit checks; however, since the bridge utilizes fully precast EREs, a nonlinear static (pushover) analysis is used. The pushover analyses define the displacement capacities of the ductile structural elements and the demands on the capacity-protected elements. The designer should ensure that the required capacity of the capacity-protected elements is provided based on the overstrength demands from the ductile elements.

CHAPTER 3. ANALYSIS MODEL

GENERAL OVERVIEW

This section provides a general description of the modeling of the bridge. The Y-axis was taken to be along the longitudinal axis of the bridge, and the Z-axis was taken to be vertical. A global view of the model is included in figure 8.

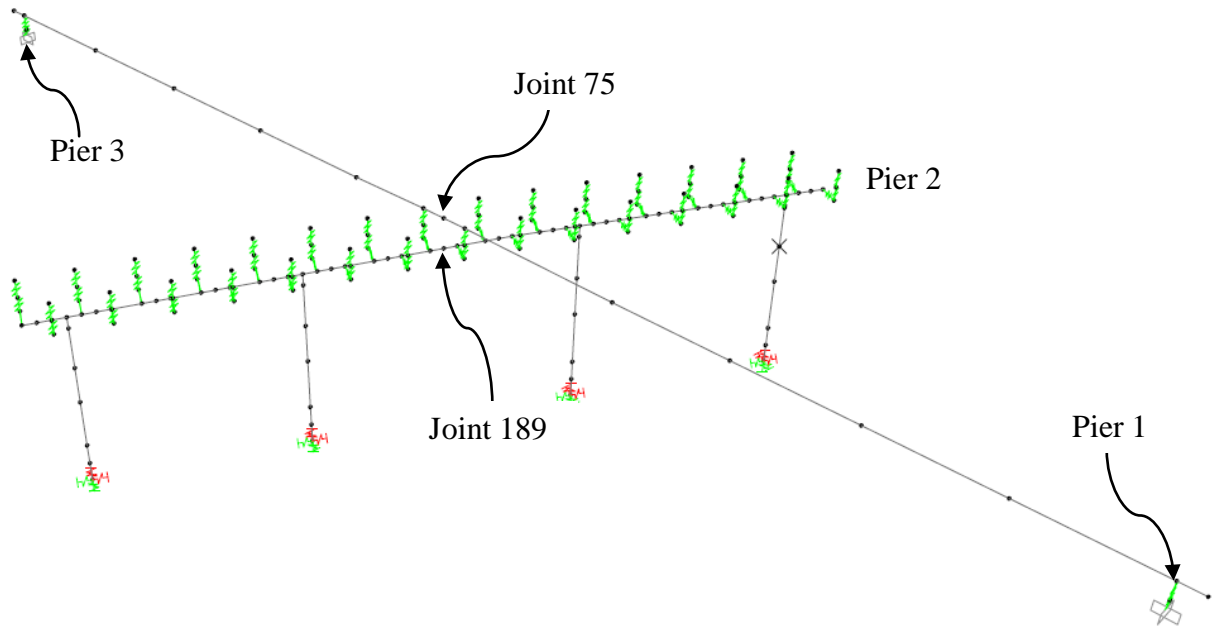


Figure 8. Diagram. Isometric view of bridge spine model.

SUPERSTRUCTURE

The bridge superstructure was modeled as a spine. All spine members were space frame members with 6 degrees of freedom at each node. All members were defined at the center of gravity of the section being modeled. The superstructure has a minimum of four members per span, as required by article 5.4.3 of the Seismic Guide Specifications. The superstructure spine properties were calculated by the use of the parallel axis theorem, and full composite action between individual girders was assumed. The modular ratio between the 4,000 psi topping and 7,500 psi girder was used to form a composite section. The masses of the diaphragms and barriers were applied to the model as point and uniform mass, respectively. Gross properties were used for the superstructure. If the superstructure was a reinforced concrete box girder, the designer would need to account for the moment of inertia and shear area modifiers specified in article 5.6 of the Seismic Guide Specifications.

CAP BEAMS

The superstructure spine was attached to the cap beam via rigid links. The rigid links were made between the center of gravity of the superstructure and the top of the cap beam (i.e., girder

bearing location). Another rigid link was made from the bearing location to the center of gravity of the cap beam. The rigid links were assigned to have zero density and mass.

The cap beams were represented by space frame members. The joints of the cap beam members were defined in elevation at the cap beam center of gravity. A joint was placed at the ends of the cap beam, at the column centerline intersections, and where the superstructure spine tied into the cap beam in plan. Additional rigid links were used to connect the cap beam joints centered over the columns to the joints located in elevation at the top of column.

Because a spine model was used, the nodes at the end of the rigid offsets to the centerline of the cap beam were constrained to each other, enforcing equal vertical displacements under gravity loading and uniform rotation of the cap beam under longitudinal seismic excitation, which ensures reasonable force distribution to the substructure components during the seismic acceleration of the model. This effectively produced a rigid cap beam. If the nodes were not constrained to each other, all of the superstructure load would be concentrated at the intersection of the superstructure spine and the cap beam, which would lead to an inaccurate force distribution, and likely inaccurate displacements.

COLUMNS

The columns were modeled by space frame members. Three members were used to connect the joints at the column top (bottom of cap beam) and column bottom (top of foundation). This satisfied the minimum required by article 5.4.3 of the Seismic Guide Specifications. The bottom-of-column joints were connected by a vertical rigid member to the centerline of the spread footing where the foundation springs were applied.

An effective moment of inertia should be used to model the ductile column members. Article 5.6.2 of the Seismic Guide Specifications specifies acceptable ways of determining the effective moment of inertia for ductile reinforced concrete members. For this design example, the effective moment of inertia was estimated using figure 5.6.2-1 of the Seismic Guide Specifications, knowing the axial dead load to the columns and anticipated longitudinal reinforcing ratio of the column. Alternatively, the effective moment of inertia can be taken as the slope of the $M-\phi$ curve between the origin and the point corresponding to the first reinforcing bar yield as follows:

1. Run a gravity load analysis to determine the dead load in each column.
2. Enter the dead load into an $M-\phi$ program.
3. Determine the slope of the $M-\phi$ curve between the point of first yield of the longitudinal reinforcing and the origin. This is equal to the product of the Young's Modulus and the effective moment of inertia of the column.
4. Divide the calculated slope by the Young's modulus.

Some computer programs allow the column properties to be specified as the product of a multiplier and the gross properties of the section. In this case, an additional step should be taken to determine the ratio of the effective inertia to the gross inertia. For reinforced concrete sections, the Young's modulus of concrete is used, and the adjustment for effective stiffness includes the combined concrete and steel section behavior, including cracking. In this design example the

column elastic properties were defined using the square cross-section, while the plastic hinges were defined using the circular cross-section at the top and bottom of the column.

FOUNDATION MODELING

Because the bridge is located in Site Class C, Foundation Modeling Method II, as specified in article 5.3.1 of the Seismic Guide Specifications, was used. This requires that springs be used to model the bridge foundations.

Spread Footings

The flexibility of the spread footings was accounted for using article 5.3.2 of the Seismic Guide Specifications and the WSDOT BDM. This resulted in foundation springs for horizontal translation, vertical translation, torsion, and rocking. Upper and lower bound values were generated to predict a soft or a stiff foundation response. The spring values are provided in table 2.

Table 2. Foundation spring properties.

	K_{soft}	K_{stiff}
Horizontal Translation	170,000 kip/ft	284,000 kip/ft
Vertical Translation	129,000 kip/ft	215,000 kip/ft
Rocking	13,519,000 kip-ft/rad	22,531,000 kip-ft/rad
Torsion	24,334,000 kip-ft/rad	40,556,000 kip-ft/rad

The analysis model used the soft footing springs to provide the maximum displacement.

Abutments

The abutments were designed and modeled to allow free superstructure translation along the longitudinal axis of the bridge and full restraint in the transverse direction.

MATERIAL MODELING

The material definitions used in the model, and the members to which they are applied, are shown in table 3.

Table 3. Material properties.

Material Name	Material	Applicable Members	Material Unit Weight
4,000psi – Deck	Concrete	Superstructure	160 pcf
4,000psi – Other	Concrete	Cap beams, columns	160 pcf
7,500psi – Girder	Concrete	Superstructure	160 pcf
A706 – Rebar	Steel	Superstructure, cap beam, columns	490 pcf

The material name for the concrete items indicates the nominal strength of the material. As stated in article 8.4 of the Seismic Guide Specifications, the use of “expected material properties” is required for the determination of the section stiffness and overstrength capacities in SDCs B and C, and it is required for the determination of section stiffness, overstrength capacities, and displacement capacities in SDC D. Table 8.4.2-1 in the Seismic Guide Specifications provides expected material properties for ASTM A706 and ASTM A605 Grade 60 reinforcing steels, and article 8.4.4 of the Seismic Guide Specifications indicates that the probable long-term expected strength of concrete is equal to 1.3 times that of the nominal concrete. These properties will be further defined in chapter 5 of this appendix.

CHAPTER 4. DEMAND ANALYSIS

GRAVITY ANALYSIS

The gravity loads included the weight of the superstructure, the cap beam, and the columns. The results from the gravity analysis should be checked against hand-calculated values before running the response spectrum analysis. Once the dead loads in the model have been verified, the effective moment of inertia of the columns may be calculated as shown below.

Column Properties:	Approx. reinforcing ratio	=	1.0 percent
	Gross area (4-ft diameter)	=	1,810 in ²
	f_c	=	4.0 ksi
Axial Loads:	Superstructure	=	2,089 kips
	Cap beam + columns	=	931 kips
	Total dead load (for 4 columns)	=	3,021 kips
	Dead load on each column	=	755 kips
	Axial load ratio	=	0.104
Moment of Inertia:	Ratio (Effective/Gross) (see figure 9)	=	0.35

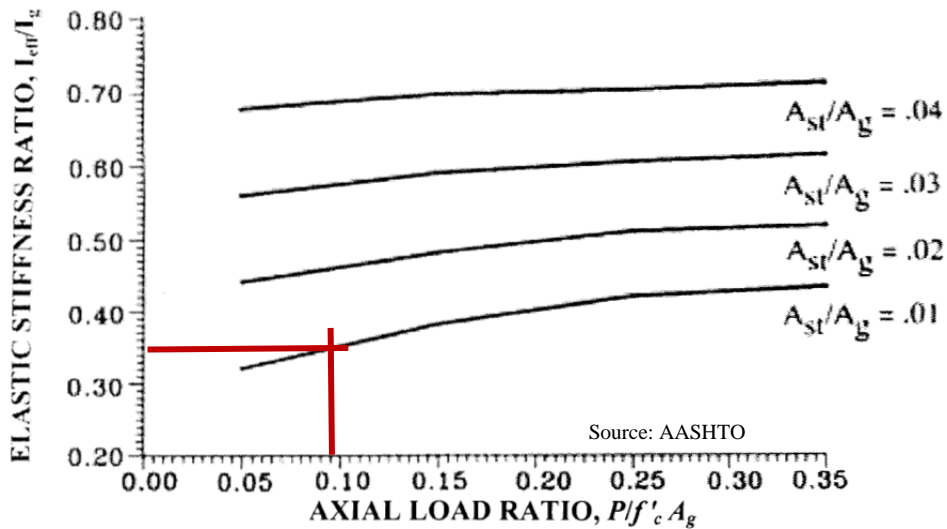


Figure 9. Graph. Effective flexural stiffness of rectangular cracked reinforced concrete sections (figure 5.6.2-1 in the Seismic Guide Specifications).

MODAL ANALYSIS

The seismic analysis combined the gravity load effects with the lateral seismic loading effects. All load factors and strength resistance factors were set equal to unity per article 3.7 of the Seismic Guide Specifications. For this example, live loading effects were not considered.

RESPONSE SPECTRUM ANALYSIS

Seismic demands were generated from a linear elastic multimodal response spectrum analysis. For this design example, a single model was used. In design, multiple models may need to be run if multiple frames exist on the bridge (i.e., tension/compression models, as defined in article 5.1.2 of the Seismic Guide Specifications for movement joints), or if liquefiable soils are present.

Per article 5.4.3 of the Seismic Guide Specifications, damping was taken to be 5 percent of critical in the analysis model, and a sufficient number of modes were included to ensure at least 90 percent participation of the total mass of the structure, with the modal response contributions combined using the complete quadratic combination (CQC) method. Vertical acceleration effects were not included in this example; however, the effects of vertical acceleration should be accounted for in essential or critical bridges in SDC D located within 6 miles of an active fault. Horizontal accelerations were aligned in the two orthogonal horizontal directions defined below:

- Bridge-Longitudinal – Along a line drawn from the intersection of the alignment line and the centerline of the first pier to the intersection of the alignment line and the centerline of the end pier.
- Bridge-Transverse – Along a line perpendicular (normal) to the bridge-longitudinal axis defined above.

To account for directional uncertainty of the earthquake, the results of the two horizontal accelerations were combined following article 4.4 of the Seismic Guide Specifications. This creates two load cases for the design displacement demand.

- Load Case 1: *100% EQ LONGITUDINAL + 30% EQ TRANSVERSE.*
- Load Case 2: *30% EQ LONGITUDINAL + 100% EQ TRANSVERSE.*

DEMANDS

Verification of Modal Information

Before the results of the response spectrum analysis are extracted from the analysis program, verification of the modal information should be made. Verification of the model was done by comparing the total weight of the structure in the model to hand-calculated values. Table 4 shows the verification of the analysis model for total weight of the structure.

Table 4. Model verification: total weight.

Pier	Weight	Model Weight	Percent Difference
1	3,269 kip	3,011 kip	-8.5
2	2,988 kip	3,237 kip	7.7
3	3,125 kip	3,145 kip	0.6
Total	9,382 kip	9,393 kip	0.1

The total base shear in the model was also compared to calculated shears based on the modal information for each direction of loading. The modal periods and mass participation were acquired from the analysis program. The associated spectral accelerations were read off of the design spectrum. The base shear was calculated using the equation in figure 10.

$$V = W \sqrt{\sum(G_i C_a)^2}$$

Figure 10. Equation. Base shear.

In figure 10:

W = Seismic weight

G_i = Modal mass participation factor

C_a = Spectral acceleration

Table 5 shows the verification of the analysis model in the transverse direction. It can be seen that mode 2 is the dominant transverse mode (closely followed by mode 4). Mode 1 is the fundamental longitudinal mode.

Table 5. Model verification: base shear transverse direction.

	Mode 1	Mode 2	Mode 3	Mode 4	Modes 5-20	Totals
Period, T_i (sec)	0.84	0.40	0.32	0.27	< 0.2	not applicable
Participation Factor, G_i	0.0012	0.329	0.0005	0.281	0.3383	0.95
Spectral acceleration, C_a (g)	0.3118	0.8419	0.8419	0.8419	0.8419	not applicable
$(G_i C_a)^2 =$	0.00	0.0767	0.00	0.0559	0.0812	0.2138

$$V = W \sqrt{\sum(G_i C_a)^2} = 0.4624$$

$W = 5,148$ kip

$V = 2,380$ kip

$V_{model} = 2,463$ kip

Difference = 3.4%

The base shear calculated above uses the square root of the sum of the squares combination method (SRSS), while the analysis program was set to use CQC. The CQC method equates to the SRSS method where structural modes are well spaced. When modes are of similar period, the CQC may differ significantly from the SRSS.

Response Spectrum Displacements

The response spectrum displacements were monitored at two joints located in the intermediate pier to determine the displacement demands for the system. For the longitudinal demand, joint 75 was monitored representing the centerline of the superstructure. For the transverse demand, joint 189 was monitored representing the centerline of the cap beam. These joints yielded the displacements shown in table 6. The load cases “Longitudinal EQ” and “Transverse EQ” do not include the directional uncertainty combination required by article 4.4 of the Seismic Guide Specifications. This should be done after the displacements are magnified per article 4.3.3 of the Seismic Guide Specifications.

Table 6. Top of column displacements—global coordinates.

Pier	Joint	Longitudinal EQ		Transverse EQ	
		X	Y	X	Y
2	75	0.247 in.	3.743 in.	n/a	n/a
2	189	n/a	n/a	0.638 in.	0.206 in.

Because the bridge is at a skew, the local (member) coordinates do not align with the global model coordinates. A simple geometric transformation converts the model output (global coordinates) to the member coordinates to determine the largest deformations parallel (X') and normal (Y') to the axis of the cap beam.

Table 7. Top of column displacements—local coordinates.

Pier	Joint	Longitudinal EQ		Transverse EQ	
		X'	Y'	X'	Y'
2	75	-1.61 in.	3.388 in.	n/a	n/a
2	189	n/a	n/a	0.457 in.	0.491 in.

Displacement Magnification

The response spectrum displacements must be magnified in accordance with article 4.3.3 of the Seismic Guide Specifications. This accounts for the fact that the equal displacement rule is not applicable for short period structures, where the inelastic demand will be larger than the elastic demand. The requirements of article 4.3.3 state that the elastic displacements determined through response spectrum analysis must be increased by the factor R_d in such cases that $T^*/T > 1.0$. See figure 11.

$$R_d = \left(1 - \frac{1}{\mu_D}\right) \frac{T^*}{T} + \frac{1}{\mu_D}$$

Figure 11. Equation. Short period amplification factor.

In figure 11:

$$T^* = 1.25 T_s = 1.25 S_{D1}/S_{DS}, \text{ seconds}$$

T = Fundamental period of the structure

μ_D = Maximum local member displacement ductility demand. (Assume $\mu_D = 3$ for SDC C; this should be checked with the actual ductility demand)

$$T_s = \frac{S_{D1}}{S_{DS}}$$

Figure 12. Equation. Short period acceleration.

$$T_s = \frac{S_{D1}}{S_{DS}} = 0.53 \text{ sec}$$

$$T_s = 1.25(0.53 \text{ sec}) = 0.66 \text{ sec}$$

Longitudinal Direction

The computed magnification for the longitudinal direction is as follows:

$$T = 0.84 \text{ sec}$$

$$\frac{T^*}{T} = \frac{0.66 \text{ sec}}{0.84 \text{ sec}} = 0.786 < 1.0$$

T^*/T is not greater than 1.0; therefore, displacements do not need to be magnified. The longitudinal displacement demands are shown in table 8.

Table 8. Top of column magnified displacements.

Pier	Joint	Longitudinal EQ	
		X'	Y'
2	75	-1.61 in.	3.39 in.

Transverse Direction

Because the mass participation is split very closely between modes 2 and 4, the magnification factor should be calculated based on the shorter period of mode 4.

The computed magnification for the transverse direction for mode 4 is as follows:

$$T = 0.28 \text{ sec}$$

$$\frac{T^*}{T} = \frac{0.66 \text{ sec}}{0.28 \text{ sec}} = 2.36 > 1.0$$

T^*/T is greater than 1.0; therefore, displacements need to be magnified. The transverse displacement demands are shown in table 9.

$$R_d = \left(1 - \frac{1}{3}\right) \frac{0.66 \text{ sec}}{0.28 \text{ sec}} + \frac{1}{3} = 1.91$$

Table 9. Top of column magnified displacements.

Pier	Joint	Transverse EQ	
		X'	Y'
2	189	0.87 in.	0.94 in.

Directional Uncertainty Combinations

Due to the inherent uncertainty in the direction of seismic excitation, article 4.4 of the Seismic Guide Specifications is used.

Load Case 1

$$100\% \text{ EQ LONGITUDINAL} + 30\% \text{ EQ TRANSVERSE}$$

$$X \text{ Displacement} = 1.0(1.61 \text{ inches}) + 0.3(0.87 \text{ inches}) = 1.87 \text{ inches}$$

$$X \text{ Displacement} = 1.87 \text{ inches}$$

$$Y \text{ Displacement} = 1.0(3.39 \text{ inches}) + 0.3(0.94 \text{ inches}) = 3.67 \text{ inches}$$

$$Y \text{ Displacement} = 3.67 \text{ inches}$$

Load Case 2

$$30\% \text{ EQ LONGITUDINAL} + 100\% \text{ EQ TRANSVERSE}$$

$$X \text{ Displacement} = 0.3(1.61 \text{ inches}) + 1.0(0.87 \text{ inches}) = 1.36 \text{ inches}$$

$$X \text{ Displacement} = 1.36 \text{ inches}$$

$$Y \text{ Displacement} = 0.3(3.39 \text{ inches}) + 1.0(0.94 \text{ inches}) = 1.95 \text{ inches}$$

$$Y \text{ Displacement} = 1.95 \text{ inches}$$

Response Spectrum Forces

The force demands from the response spectrum analysis are elastic forces. These forces will not be used in this example because the bridge is located in SDC C, which requires the use of the plastic overstrength force demands. If the bridge were in SDC B, the smaller of the elastic and the plastic overstrength demands could be used to design the bridge structural components.

CHAPTER 5. CAPACITY ANALYSIS

The capacity analysis used in this example consisted of a nonlinear static pushover analysis. The pushover models were generated from the global linear elastic response spectrum model modified to include plastic hinges at the top and bottom of each pier. Due to the column detailing, elastic column properties were based on the square cross-section, while the plastic hinge properties were based on the circular cross-section included at the top and the bottom of the column. The method of calculating the plastic hinge moment curvature relationships and analytical plastic hinge length calculations are discussed in this chapter.

The pier displacement capacity was evaluated in the pier transverse and longitudinal directions independently. The pier transverse and longitudinal directions are defined as follows:

- Pier-Longitudinal: Perpendicular to the pier centerline.
- Pier-Transverse: Parallel to the pier centerline.

The local axis for the pier was defined following the pier longitudinal and transverse definitions to extract the appropriate displacement values from the model.

A pushover model was created for the intermediate pier to define the pier transverse and longitudinal seismic displacement capacities. The pier pushover models included the unfactored dead load of the structural components and nonstructural attachments (DC) and dead load of the wearing surfaces and utilities (DW) superstructure dead load pier reactions from the global analysis model. The pushover analyses were run ignoring P- Δ effects. The displacement capacity of each pier was defined as when the first column hinge within the pier reached an ultimate curvature limit defined in article 8.5 of the Seismic Guide Specifications.

PLASTIC HINGE DEFINITIONS

There are three input values required before a plastic hinge can be assigned to the capacity analysis model. These are the plastic hinge length, the plastic hinge moment curvature (M- ϕ) relationship for a given axial load, and the plastic hinge moment-axial force (P-M) interaction curve for incipient failure conditions.

Plastic Hinge Lengths

The analytical plastic hinge lengths L_p were calculated in accordance with article 4.11.6 of the Seismic Guide Specifications. See figure 13.

$$L_p = 0.08L + 0.15f_{ye}d_{bl} \geq 0.3f_{ye}d_{bl} + G_f$$

Figure 13. Equation. Analytical plastic hinge length.

In figure 13:

L = Length of column from point of maximum moment to the point of moment contraflexure (inches)—see figure 14

f_{ye} = Expected yield strength of longitudinal reinforcing steel (68 ksi for A706 steel; see Seismic Guide Specifications table 5.1.2.1.1)

d_{bl} = Nominal diameter of longitudinal column reinforcing steel bars (inches)

G_f = Gap between the isolated flare and the soffit of the cap beam or the top of foundation (inches)

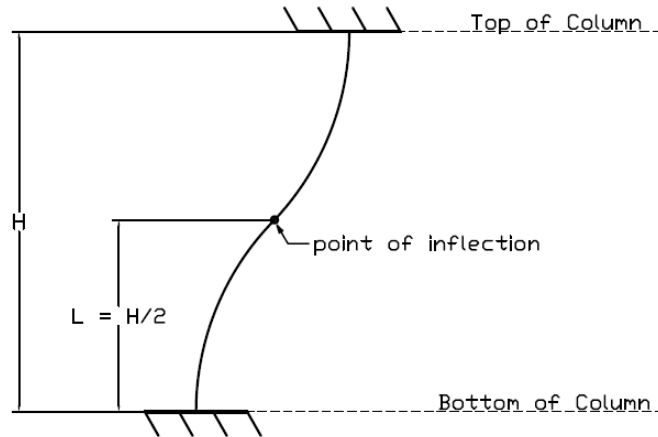


Figure 14. Graph. Column length definitions.

The example column will be designed with No. 14 longitudinal column reinforcing steel bars, where $d_{bl} = 1.693$ inches. Because the columns are restrained against rotation in both the longitudinal and transverse directions, the column will go into double curvature regardless of the direction of loading. Therefore, the plastic hinge lengths will be equal and can be calculated using the shortest column height ($H = 19$ ft 2 inches), as follows:

$$L = \frac{H}{2} = \frac{19.17 \text{ ft}}{2} = 115 \text{ in.} \quad (\text{column in double curvature})$$

$$L_p = 0.08(115 \text{ in.}) + 0.15(68 \text{ ksi})(1.693 \text{ in.}) = 26.47 \text{ in.}$$

greater than or equal to

$$L_p = 0.3 (68 \text{ ksi})(1.693 \text{ in.}) + 3 \text{ in.} = 37.5 \text{ in.}$$

Therefore, use:

$$L_p = 37.5 \text{ in.}$$

Moment-Curvature Relationships

In the analysis model, the column moment-curvature responses were approximated as elastic perfectly plastic. Sectional responses were developed for multiple axial loads to account for associated changes in moment capacity and ultimate curvature limits. The actual moment-curvature relationship used by the analysis program interpolated between the defined curves

based upon the axial load in the member of concern. Similarly, the moment capacity assigned to the curve comes from interpolation of the P-M interaction surface.

The plastic moment capacities of the columns were determined from a fiber discretized cross-sectional analysis based on strain compatibility using commercially available software. Expected material strengths were used to calibrate the constitutive relations within the cross section. Both the confined concrete properties and the strain-hardening effects of the longitudinal reinforcement were accounted for, and ultimate curvature capacity of the section was determined based on material strain limits.

Note that the material properties, column curvature limits, and column P-M curve shown in the following pages are specific to a 4-foot-diameter circular column with 8 No.14 longitudinal bars and a No. 5 spiral at 4-inch pitch. The column design is a critical step in the development of the seismic model. The design chosen for the example satisfies the minimum strength requirements of the Seismic Guide Specifications, and it is assumed to satisfy the minimum requirements of the force-based Bridge Design Specifications.

Mander's confined concrete model was used to define the concrete stress-strain relationship.⁽⁶⁾ This is in accordance with article 8.4.4 of the Seismic Guide Specifications. The unconfined concrete compressive strain at the maximum compressive stress was taken to be 0.002, and the ultimate unconfined concrete compressive strain at spalling was taken to be 0.005. The effective concrete compressive strength was set to be equal to 1.3 times the 28-day compressive strength. The 28-day concrete compressive strength was taken to be 4,000 psi. Figure 15 shows the unconfined and confined concrete stress-strain relationships for the columns.

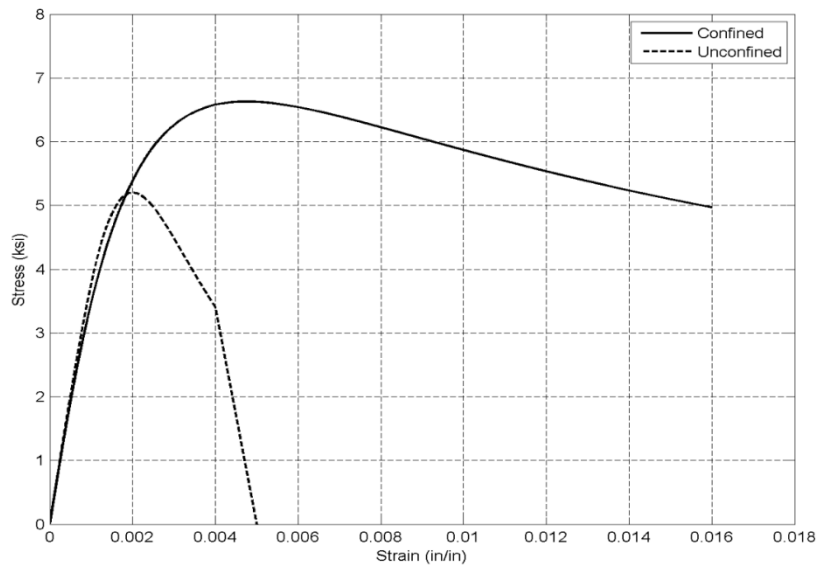


Figure 15. Graph. Column concrete stress-strain relationships.

The Raynor model was used to define the reinforcing steel stress-strain relationship.⁽⁷⁾ The reinforcing steel properties were taken to be ASTM A706, Grade 60. The parameters used to define the ASTM A706 stress-strain relationship are shown in table 10, and the associated curve is shown in figure 16.

Table 10. ASTM A706, Grade 60 properties.

Parameter	Bar Size	Value
Modulus of Elasticity	No. 3 - No. 18	29,000 ksi
Minimum Yield Strength	No. 3 - No. 18	60.0 ksi
Expected Yield Strength	No. 3 - No. 18	68.0 ksi
Expected Tensile Strength	No. 3 - No. 18	95.0 ksi
Expected Yield Strain	No. 3 - No. 18	0.0023
Onset of Strain Hardening	No. 3 - No. 8	0.015
	No. 9	0.0125
	No. 10 - No. 11	0.0115
	No. 14	0.0075
	No. 18	0.005
Reduced Ultimate Tensile Strain	No. 4 - No. 10	0.09
	No. 11 - No. 18	0.06
Ultimate Tensile Strain	No. 4 - No. 10	0.12
	No. 11 - No. 18	0.09

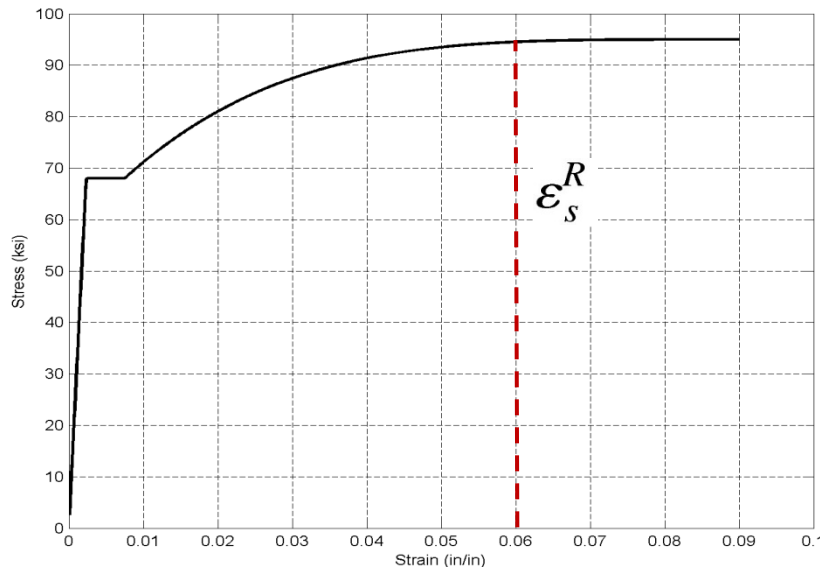


Figure 16. Graph. ASTM A706 reinforcement stress-strain relationship.

The curvature capacity of the plastic hinges was defined as the first occurrence of either compression failure of confined concrete, or fracture of longitudinal reinforcement. The curvature at effective yield and ultimate conditions are shown in table 11 for various axial loads. The moment curvature response is idealized as a bilinear curve based on the provisions in article 8.5 in the Seismic Guide Specifications. The elastic portion of the curve is the secant from the origin to the point of first yield within the column. The plastic portion of the curve is set by balancing the areas between the actual and idealized curves for curvatures beyond the point of first yield. This simplification is used to reduce computational cost within the pushover analysis

and allow the nonlinear plastic hinge response to be modeled in conventional software. An example moment-curvature response is shown in figure 17.

Table 11. Curvature limits.

Axial Load (kips)	ϕ at Effective Yield (rad/inch)	ϕ at Ultimate (rad/inch)
-1,224	Tension Limit	
-1,000	8.22e-5	0.0016
-500	1.33e-4	0.0018
0	1.13e-4	0.0019
1,000	1.14e-4	0.002
2,000	1.11e-4	0.0011
3,000	9.03e-5	0.0009
4,000	7.28e-5	0.0008
5,500	6.26e-5	0.0006
10,940	Compression Limit	

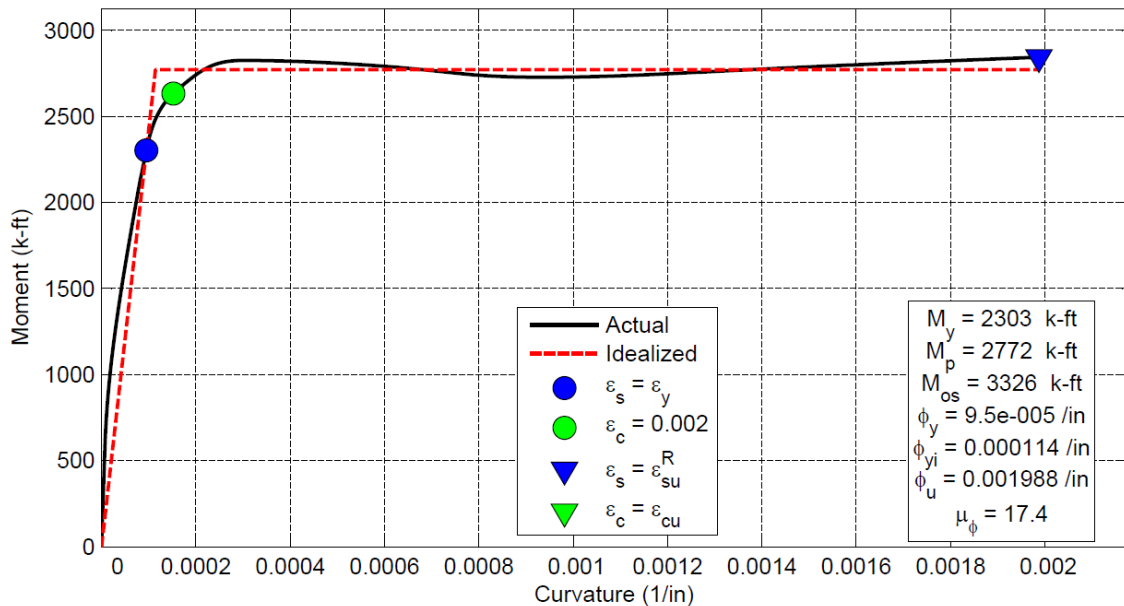


Figure 17. Graph. Typical moment-curvature relationship (axial load = 1,000 kips).

Axial Force-Moment Interaction Curves

The P-M interaction curve for the column plastic hinges was generated by taking the moment values as the plastic capacities from the idealized moment-curvature response for each given axial load. As the columns were circular within the plastic hinge region, the P-M interaction was taken to be symmetric. In the case of rectangular columns, biaxial bending affects should be considered. The P-M interaction curve is shown in figure 18. The P-M interaction curve was entered into the analysis program to define the behavior of the plastic hinges at the top and bottom of the columns. If reinforcement or column sections were to differ at the top and bottom

of the column, separate P-M interaction curves would be required for the top and bottom plastic hinges. In this design example, the reinforcement and column sections were the same at the top and bottom of the column, so only one P-M interaction curve was used.

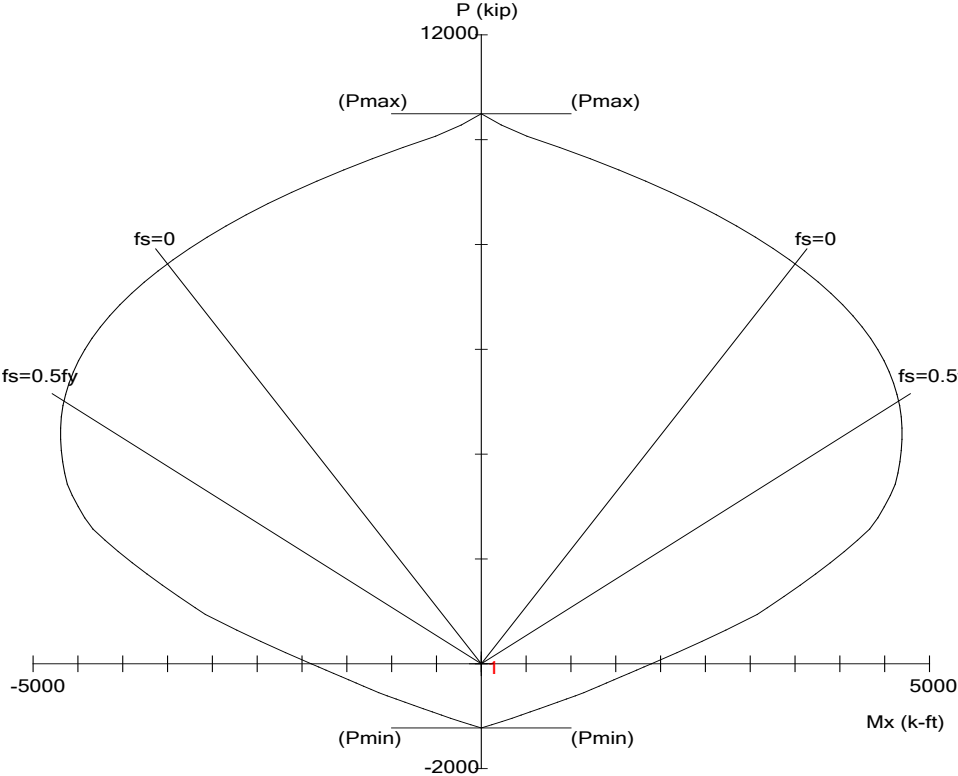


Figure 18. Diagram. Column P-M interaction curve.

Plastic Hinge Assignment

How the plastic hinges are specifically assigned to the model depends on the software being used. Before the hinges can be assigned to the model, though, the relative location of the plastic hinge needs to be determined. Plastic hinges will be placed at the top and bottom of the columns. In some bridge configurations, the structure will behave differently in the longitudinal and transverse directions, so different plastic hinges need to be defined for each load direction. The plastic hinge is placed at mid-height of the analytical plastic hinge length, or $L_p/2$ away from the cap beam soffit or the top of the spread footing. Realistically, part of the predicted plastic hinge length includes strain penetration into the footing or the cap beam; therefore, the plastic hinge could be placed closer to the column-footing or column-cap beam interface. Thus, placing the concentrated hinge $L_p/2$ away from the interface leads to a low, and therefore conservative, estimate of the displacement capacity. As the columns will go into double curvature for loading in both the longitudinal and transverse directions, the hinge distance from connecting element (footing or cap beam) is equal to $L_p/2$, or 18.8 inches.

CAPACITIES

Pushover Displacement Capacities

The pushover base shear versus displacement relationship is shown in figures 19 and 20 for the longitudinal and transverse pushover analyses, respectively. The figures show the displacement demands from the two orthogonal load combinations specified in chapter 4. The displacements shown in the pushover curves include the effects of the foundation springs. As stated in article 5.3.1 of the Seismic Guide Specifications, if foundation springs are included in the displacement demand model, the springs are required to be present for the determination of displacement capacity.

In the transverse pushover, there is more pronounced rounding in the plastification transition than in the longitudinal case, due to the changes in column axial load from frame action in the multicolumn pier.

In the figures, the pushover curves are shown to terminate at the first failed plastic hinge. Some pushover analysis software packages may provide additional points indicating failures of subsequent hinges, but the additional points are unnecessary as the displacement capacity is taken at the displacement associated with the first failed plastic hinge. The displacement capacities are shown in table 12.

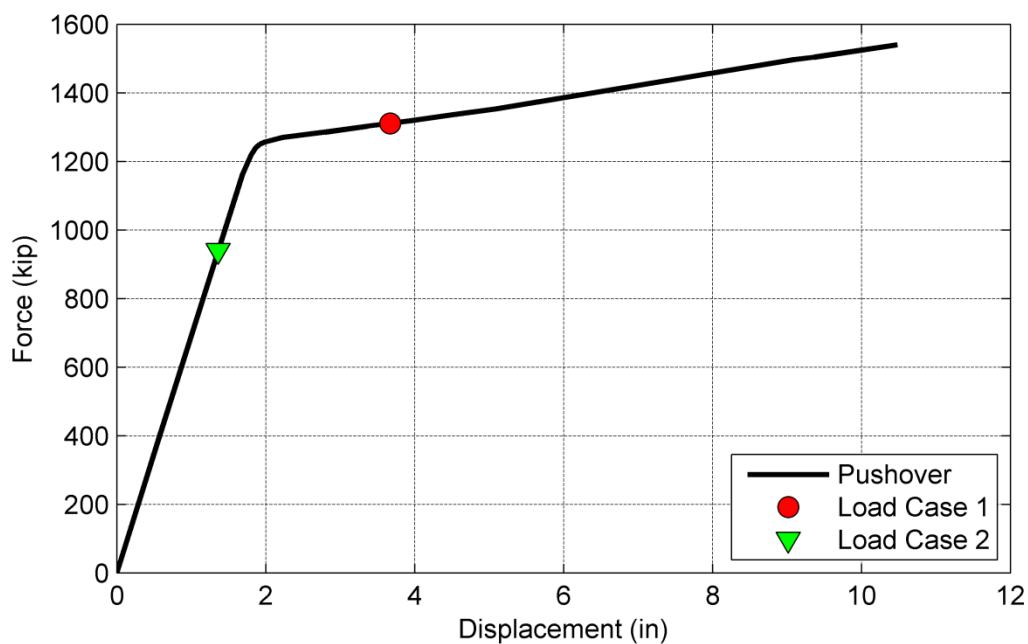


Figure 19. Graph. Longitudinal direction pushover curve.

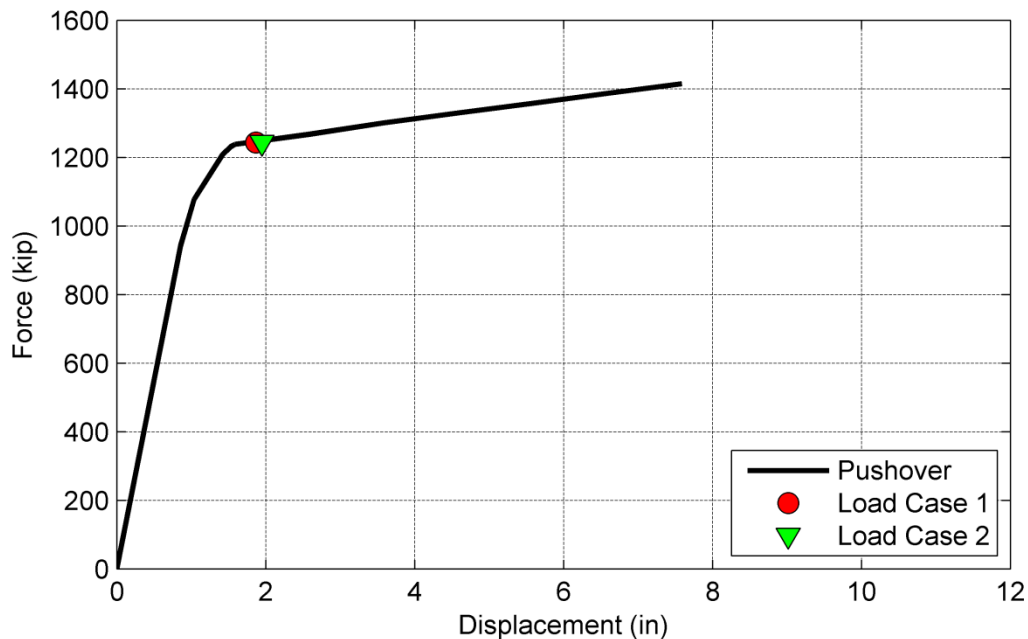


Figure 20. Graph. Transverse direction pushover curve.

Table 12. Pier displacement capacities.

Pier	Joint	Longitudinal PO		Transverse PO	
		X	Y	X	Y
2	189	0.0 in.	10.5 in.	7.56 in.	0.0 in.
2	75	0.0 in.	10.5 in.	7.56 in.	0.0 in.

The capacities determined by the pushover analysis are greater than the magnified displacement demands, as discussed in chapter 4, and are thus satisfactory.

Inelastic Column Moment and Shear Demands

In Type I structures, the substructure components act as fuses to limit the seismically induced forces on the superstructure and foundation components (i.e., capacity-protected elements). In this design example, the fuses are the plastic hinges that are allowed to form at the top and bottom of the columns. The member overstrength design forces are the plastic capacities of the fuses multiplied by a strength magnification factor. The design forces for a bent with two or more columns must be calculated for displacements in the plane of the bent and perpendicular to the bent using expected material properties.

In-Plane Pier Design Forces

The plastic overstrength demands were determined following the procedures of article 4.11.4 of the Seismic Guide Specifications. Article 4.11.4 gives four steps to calculate the plastic hinging forces for bents with two or more columns within the plane of the bent. In this design example, the calculations used to determine the overstrength demands from the column plastic hinging are omitted, as they are not unique to a fully precast integral bent system. The axial, flexural, and

column shear demands are shown in table 13. The axial demands are asymmetric due to the overturning axial forces generated due to frame action within the bent.

Table 13. In-plane pier design forces.

	South Column	Center South Column	Center North Column	North Column
Axial Load (kip)	797	956	800	391
Length (ft)	19.17	20.1	20.83	20.75
Overstrength Moment (k-ft)	3,422	3,626	3,426	2,802
Column Shear (kip)	357	360.8	328.9	270.1

Out-of-Plane Pier Design Forces

Article 4.11.3 of the Seismic Guide Specifications covers plastic hinging perpendicular to the plane of the bent. The shear associated with plastic hinging is the sum of the plastic moment at the top and the bottom of the column, divided by the column height. In this example, the intermediate calculations are omitted, and the overstrength forces are as shown in table 14.

Table 14. Out-of-plane pier design forces.

	South Column	Center South Column	Center North Column	North Column
Axial Load (kip)	594	878	878	594
Length (ft)	19.17	20.1	20.83	20.75
Overstrength Moment (k-ft)	3,119	3,528	3,528	3,119
Column Shear (kip)	325.4	351.0	338.7	300.6

Once the plastic overstrength demands of the ductile elements are determined, the nominal shear capacity of the ductile elements must be checked to ensure the shear can be transferred to the capacity-protected elements. Assuming this is satisfied, the designer must use the plastic overstrength demands to design the capacity protected structural components. This is addressed in the next chapter.

CHAPTER 6. DESIGN CHECKS

DISPLACEMENT CAPACITY-TO-DEMAND RATIO

Each bent must have a displacement capacity-to-demand ratio greater than unity as specified in article 4.8 of the Seismic Guide Specifications. The requirement is as shown in figure 21, and the calculations for this design example are shown in table 15.

$$\Delta_D^L < \Delta_C^L$$

Figure 21. Equation. Displacement capacity-to-demand ratio requirement.

In figure 21:

Δ_D^L = Displacement demand taken along the local principal axis of the ductile member, inches

Δ_C^L = Displacement capacity taken along the local principal axis corresponding to Δ_D^L of the ductile member, inches

Table 15. Displacement capacity-to-demand check.

Case	Longitudinal Displacements	Transverse Displacements
Capacity	10.5 inches	7.6 inches
Demand	3.67 inches	1.87 inches
C/D	2.86 OK!	4.06 OK!

MEMBER DUCTILITY

The individual ductile members of the structure must satisfy the member ductility requirements of article 4.9 of the Seismic Guide Specifications. The member ductility demand may be computed as shown in figure 22.

$$\mu_D = 1 + \frac{\Delta_{pd}}{\Delta_{yi}}$$

Figure 22. Equation. Displacement ductility demand.

In figure 22:

Δ_{yi} = Idealized yield displacement corresponding to the idealized yield curvature, ϕ_{yi} , inches (see figure 23)

Δ_{pd} = Plastic displacement demand, inches (see figure 24)

$$\Delta_{yi} = \frac{\phi_{yi}L^2}{3}$$

Figure 23. Equation. Idealized yield displacement.

$$\Delta_{pd} = \phi_{pd}L_p \left(L - \frac{L_p}{2} \right) = \theta_{pd} \left(L - \frac{L_p}{2} \right)$$

Figure 24. Equation. Plastic displacement demand.

In figures 23 and 24:

ϕ_{yi} = Effective curvature at yield from moment curvature software

ϕ_{pd} = Plastic curvature demand associated with plastic rotation demand, defined as shown in figure 25.

$$\phi_{pd} = \frac{\theta_{pd}}{L_p}$$

Figure 25. Equation. Plastic curvature demand.

θ_{pd} = Plastic rotation (hinge rotation from pushover model at the demand displacement)

L = Distance from point of maximum moment to point of inflection; (total column height for single curvature, half of column height for double curvature)

L_p = Plastic hinge length

For a multiple column bent, the individual member displacement ductility demand, μ_D , must be less than or equal to 6, as stipulated in article 4.9 of the Seismic Guide Specifications. A ductility demand less than unity would indicate that the plastic hinges have not yielded and the column is remaining elastic.

As the columns in this bridge will always go into double curvature under a lateral load, the distance from the point of maximum moment to the inflection point will be assumed to equal half of the column height.

Longitudinal Direction

The calculated individual member longitudinal displacement ductility demand for the plastic hinge at the bottom of the south column is calculated as follows:

$$\theta_{pd} = 0.0102 \text{ rad}$$

$$\Delta_{yi} = \frac{\phi_{yi}L^2}{3} = \frac{(0.000113 \text{ rad/inch})(115 \text{ inches})^2}{3} = 0.50 \text{ inches}$$

$$\Delta_{pd} = \theta_{pd} \left(L - \frac{L_p}{2} \right) = 0.0102 \text{ rad} \left(115 \text{ inches} - \frac{37.5 \text{ inches}}{2} \right) = 0.98 \text{ inches}$$

$$\mu_D = 1 + \frac{\Delta_{pd}}{\Delta_{yi}} = 1 + \frac{0.98 \text{ inches}}{0.50 \text{ inches}} = 2.96 \leq 6.0$$

The calculated individual member ductility demands for the top and bottom column hinges are presented in tables 16 and 17, respectively, for all columns. The difference in the axial load on the top and bottom plastic hinges is the self-weight of column.

Table 16. Ductility demands, longitudinal direction—top hinge.

	South Column	Center South Column	Center North Column	North Column
P_{DL} (kip)	543	827	827	543
θ_{pd} (rad)	0.0102	0.00952	0.00902	0.00895
ϕ_{yi} (rad/in)	0.000113	0.000113	0.000113	0.000113
L (inch)	115	120.5	125	124.5
Δ_{yi} (inch)	0.50	0.55	0.59	0.58
Δ_{pd} (inch)	0.98	0.97	0.96	0.95
Δ_d (inch)	1.48	1.52	1.55	1.53
μ_D	2.97 OK!	2.77 OK!	2.63 OK!	2.62 OK!

Table 17. Ductility demands, longitudinal direction—bottom hinge.

	South Column	Center South Column	Center North Column	North Column
P_{DL} (kip)	594	878	878	594
θ_{pd} (rad)	0.0102	0.00953	0.00888	0.00879
ϕ_{yi} (rad/in)	0.000113	0.000113	0.000113	0.000113
L (inch)	115	120.5	125	124.5
Δ_{yi} (inch)	0.50	0.55	0.59	0.58
Δ_{pd} (inch)	0.98	0.97	0.94	0.93
Δ_d (inch)	1.48	1.52	1.53	1.51
μ_D	2.96 OK!	2.77 OK!	2.60 OK!	2.59 OK!

Transverse Direction

In the transverse direction, the multiple-column bent ductility requirements must be met. The calculated individual member ductility demands for the top and bottom column hinges are presented in tables 18 and 19, respectively, for all columns. The following is an example calculation for the bottom of column hinge in the south column:

$$\theta_{pd} = 0.00434 \text{ rad}$$

$$\Delta_{yi} = \frac{\phi_{yi} L^2}{3} = \frac{(0.000113 \text{ rad/inch})(115 \text{ inches})^2}{3} = 0.50 \text{ inches}$$

$$\Delta_{pd} = \theta_{pd} \left(L - \frac{L_p}{2} \right) = 0.00434 \text{ rad} \left(115 \text{ inches} - \frac{37.5 \text{ inches}}{2} \right) = 0.42 \text{ inches}$$

$$\mu_D = 1 + \frac{\Delta_{pd}}{\Delta_{yi}} = 1 + \frac{0.42 \text{ inches}}{0.50 \text{ inches}} = 1.84 \leq 6.0$$

Table 18. Ductility demands, transverse direction—top hinge.

	South Column	Center South Column	Center North Column	North Column
P_{DL} (kip)	746	904	748	339
θ_{pd} (rad)	0.00725	0.00654	0.00589	0.00581
ϕ_{yi} (rad/in)	0.000113	0.000114	0.000113	0.000111
L (inch)	115	120.5	125	124.5
Δ_{yi} (inch)	0.50	0.55	0.59	0.57
P_{DL} (kip)	0.70	0.67	0.63	0.61
θ_{pd} (rad)	1.20	1.22	1.21	1.19
ϕ_{yi} (rad/in)	2.40 OK!	2.21 OK!	2.06 OK!	2.07 OK!

Table 19. Ductility demands, transverse direction—bottom hinge.

	South Column	Center South Column	Center North Column	North Column
P_{DL} (kip)	797	956	800	391
θ_{pd} (rad)	0.00434	0.00358	0.00281	0.00250
ϕ_{yi} (rad/in)	0.000113	0.000114	0.000113	0.000111
L (inch)	115	120.5	125	124.5
Δ_{yi} (inch)	0.50	0.55	0.59	0.57
Δ_{pd} (inch)	0.42	0.36	0.30	0.26
Δ_d (inch)	0.92	0.92	0.89	0.84
μ_D	1.84 OK!	1.66 OK!	1.51 OK!	1.46 OK!

COLUMN PLASTIC HINGE SHEAR CAPACITY-TO-DEMAND RATIO

The column shear capacity requirements are specified in article 8.6 of the Seismic Guide Specifications. The equations shown in this section apply only to shear in the plastic hinging region. The column outside of the plastic hinging region must be checked for shear capacity by the methods shown in the Bridge Design Specifications. Bridge Design Specification calculations are not included in this example.

The design shear capacity is the sum of the steel and shear components multiplied by a strength reduction factor, as shown in figure 26.

$$V_u \leq \phi(V_c + V_s)$$

Figure 26. Equation. Shear capacity requirement.

Figures 27 through 33 show the calculation of the concrete shear component.

$$V_c = v_c A_e$$

Figure 27. Equation. Concrete shear resistance.

in which:

$$A_e = 0.8A_g$$

Figure 28. Equation. Effective area.

and if the column is in compression:

$$v_c = 0.32\alpha' \left(1 + \frac{P_u}{2A_g} \right) \sqrt{f'_c} \leq \min \begin{cases} 0.11 \sqrt{f'_c} \\ 0.047\alpha' \sqrt{f'_c} \end{cases}$$

Figure 29. Equation. Concrete shear resistance if the column is in compression.

Where:

$$0.3 \leq \alpha' = \frac{f_s}{0.15} + 3.67 - \mu_D \leq 3.0$$

Figure 30. Equation. Concrete shear stress adjustment factor.

$$f_s = \rho_s f_{yh} \leq 0.35$$

Figure 31. Equation. Calculating f_s .

$$\rho_s = \frac{4A_{sp}}{sD'}$$

Figure 32. Equation. Volumetric ratio of transverse steel.

A_g = Gross area of the member cross-section, in²

P_u = Ultimate compressive force acting on the section, kips

f_{yh} = Nominal yield strength of transverse reinforcing, ksi

μ_D = Maximum member displacement ductility ratio (for SDC C $\mu_D = 3$)

A_{sp} = Area of spiral or hoop reinforcing bar, in²

D' = Core diameter of column from center of spiral or hoop, inches

s = Pitch of spiral or spacing of hoops/ties, inches

If the column is in tension:

$$v_c = 0$$

Figure 33. Equation. Concrete shear resistance if the column is in tension.

Figure 34 shows the calculation of the steel shear component.

$$V_s = \frac{\pi}{2} \left(\frac{nA_{sp}f_{yh}D'}{s} \right)$$

Figure 34. Equation. Steel shear resistance.

In figure 34:

n = Number of individual interlocking spiral or hoop core sections

f_{yh} = Nominal yield stress of the transverse reinforcing, ksi

Longitudinal Direction

In the longitudinal direction, the anticipated change in axial loads is quite small. The axial load is approximately equal to the dead load. The associated shear capacity (calculated according to article 8.6.2 of the Seismic Guide Specifications) for an exterior column is calculated as shown below.

Concrete shear component:

$$\rho_s = \frac{4(0.31 \text{ in}^2)}{(4 \text{ in.})(40 \text{ in.})} = 0.0077$$

$$f_s = \rho_s f_{yh} = 0.0077(60 \text{ ksi}) = 0.46 \geq 0.35 \rightarrow \text{Use } f_s = 0.35$$

Use $\mu_D = 2.97$ which is the larger ductility demand between the top and the bottom plastic hinges.

$$\alpha_s = \frac{f_s}{0.15} + 3.67 - \mu_D = \frac{0.35}{0.15} + 3.67 - 2.97 = 3.03$$

$$v_c = 0.032\alpha' \left(1 + \frac{P_u}{2A_g} \right) \sqrt{f'_c} = 0.032(3.03) \left(1 + \frac{594 \text{ kips}}{2(1,809 \text{ in}^2)} \right) \sqrt{4 \text{ ksi}} = 0.225 \text{ ksi}$$

$$v_{c,max} = 0.11 \sqrt{f'_c} = 0.11 \sqrt{4 \text{ ksi}} = 0.22 \text{ ksi}$$

$$v_{c,max} = 0.047\alpha' \sqrt{f'_c} = 0.047(3.13) \sqrt{4 \text{ ksi}} = 0.295 \text{ ksi}$$

$$A_e = 0.8A_g = 0.8(1,809 \text{ in}^2) = 1,448 \text{ in}^2$$

$$V_c = v_c A_e = 0.22 \text{ ksi}(1,809 \text{ in}^2) = 318.6 \text{ kip}$$

Steel shear component:

$$V_s = \frac{\pi}{2} \left(\frac{n A_{sp} f_{yh} D'}{s} \right) = \frac{\pi}{2} \left(\frac{(0.31 \text{ in}^2)(60 \text{ ksi})(40.375 \text{ inches})}{4 \text{ inches}} \right) = 295 \text{ kip}$$

Column shear strength:

$$\phi V_n = \phi (V_c + V_s) = 0.9(318.6 \text{ kip} + 295 \text{ kip}) = 552 \text{ kip}$$

The capacity-to-demand ratio for the longitudinal plastic hinge shear check is shown in table 20 for both interior and exterior columns. The columns are satisfactory for longitudinal shear at the plastic hinge.

Table 20. Longitudinal hinge shear C/D check.

	South Column	Center South Column	Center North Column	North Column
Capacity	552 kip	552 kip	552 kip	552 kip
Demand	325.4 kip	351.0 kip	338.7 kip	300.6 kip
C/D	1.69 OK!	1.57 OK!	1.62 OK!	1.84 OK!

Check the maximum shear reinforcement requirement according to the Seismic Guide Specifications, article 8.6.4, as shown below:

$$V_s \leq 0.25 \sqrt{f'_c} A_g$$

$$V_s \leq 0.25 \sqrt{4 \text{ ksi}} (1,448 \text{ in}^2) = 724 \text{ kip}$$

The provided shear reinforcement results in a capacity that is less than the maximum allowable shear capacity. Check the minimum shear reinforcement ratio required, according to the Seismic Guide Specifications, article 8.6.5:

$$\rho_s \geq 0.005$$

The shear reinforcement ratio is calculated above to be 0.0077. Thus, the minimum shear reinforcement requirement is satisfied.

Transverse Direction

In the transverse direction, the outer columns will be checked for both the minimum and maximum expected axial loads due to the cyclic effects of the seismic loading. Following the example shown in the preceding section for the longitudinal loading, the associated shear capacities are calculated to be:

- South Column: $\phi V_n = 483$ kips.
- Center South Column: $\phi V_n = 490$ kips.
- Center North Column: $\phi V_n = 483$ kips.
- North Column: $\phi V_n = 458$ kips.

The capacity-to-demand ratio for the transverse hinge shear check is shown in table 21. The columns are satisfactory for transverse shear at the hinge.

Table 21. Transverse hinge shear C/D check.

	South Column	Center South Column	Center North Column	North Column
Capacity	483 kip	490 kip	483 kip	458 kip
Demand	357 kip	360.8 kip	328.9 kip	270.1 kip
C/D	1.35 OK!	1.36 OK!	1.47 OK!	1.7 OK!

P-Δ EFFECTS

The capacity analysis conducted as part of this design example did not include P-Δ effects, and thus, for a Type I structure, the requirements of article 4.11.5 of the Seismic Guide Specifications must be satisfied or a nonlinear time history analysis, including P-Δ effects, must be performed. For reinforced concrete columns, the requirement is as shown in figure 35.

$$P_{dl}\Delta_r \leq 0.25M_p$$

Figure 35. Equation. P-Δ check.

In figure 35:

P_{dl} = Unfactored dead load acting on the column, kips

Δ_r = Relative lateral offset between the point of inflection and the furthest end of the plastic hinge, inches

M_p = Idealized plastic moment capacity of reinforced concrete column based upon expected material properties, kip-in.

In this design example:

$$\begin{aligned} \Delta_r &= 3.67 \text{ inch} / 2 = 1.84 \text{ inch (longitudinal – double curvature)} \\ &= 1.95 \text{ inch} / 2 = 0.975 \text{ inch (transverse – double curvature)} \end{aligned}$$

Tables 22 and 23 illustrate that the requirement above is satisfied for all axial load and moment pairs. Thus, P-Δ effects may be neglected.

If this step is performed at an initial stage to set initial column size prior to plastic analysis (and development of the M_p used in the equation), the nominal moment capacity with expected properties M_{ne} used to check the minimum lateral strength of the column can be used as an approximate value in place of M_p , with the intention to finish a more accurate M_p check after plastic analysis is completed.

Table 22. P- Δ check—transverse.

	South Column	Center South Column	Center North Column	North Column
Δ_r	0.975 inch	0.975 inch	0.975 inch	0.975 inch
P_{dl}	797 kip	956 kip	800 kip	391 kip
M_p	3,422 kip-ft	3,626 kip-ft	3,426 kip-ft	2,802 kip-ft
$P_{dl}\Delta_r$	65 kip-ft	78 kip-ft	65 kip-ft	31.8 kip-ft
$0.25 M_p$	855 kip-ft	906 kip-ft	856 kip-ft	700 kip-ft
Incl. P-Δ	NO	NO	NO	NO

Table 23. P- Δ check—longitudinal.

	South Column	Center South Column	Center North Column	North Column
Δ_r	1.84 inch	1.84 inch	1.84 inch	1.84 inch
P_{dl}	594 kip	878 kip	878 kip	594 kip
M_p	3,119 kip-ft	3,528 kip-ft	3,528 kip-ft	3,119 kip-ft
$P_{dl}\Delta_r$	91 kip-ft	135 kip-ft	135 kip-ft	91 kip-ft
$0.25 M_p$	780 kip-ft	882 kip-ft	882 kip-ft	780 kip-ft
Incl. P-Δ	NO	NO	NO	NO

SUPPORT LENGTH

The minimum support length requirements are specified in article 4.12.2 for SDCs A, B, and C, and article 4.12.3 for SDC D. The minimum support length must be provided for girders supported on an abutment, bent cap, pier wall, or in-span hinge, where the girder may displace independently from its support. In this design example, the girder ends are supported by bearing pads at the abutments. This allows the structure to displace freely in the longitudinal direction. Girder shear blocks are provided adjacent to each girder to resist any transverse displacement of the girders at each abutment. The support length was calculated to be 13.3 inches.

CAPACITY-PROTECTED MEMBER CAPACITIES

Article 8.9 of the Seismic Guide Specifications states the requirements of capacity-protected members. Capacity-protected members consist of footings, bent caps, and integral superstructure elements adjacent to plastic hinge locations. Capacity-protected elements should be designed to remain essentially elastic when the ductile elements reach their plastic overstrength capacity. Article 8.9 of the Seismic Guide Specifications requires expected material properties to be used in establishing the capacity of the capacity-protected members. In the sections that follow, the capacities are compared to the demands resulting from the plastic overstrength forces defined earlier in the example. The following is a list of the structural member capacities calculated as part of this example:

- Superstructure.
- Transverse shear blocks.
- Prestressed girder anchorage.
- Cap beam.
- Column-to-cap beam connection.
- Column splices.
- Spread footing.
- Socket connection of column to spread footing.

It should be noted that all structural member capacities should be calculated during actual design. For the sake of this example, the list above was chosen for illustration purposes.

Superstructure

The superstructure should be checked for flexure and shear, as would typically be done as part of any other load case. This should be done for both the transverse and longitudinal seismic event. The superstructure should be designed to remain essentially elastic under the overstrength demands from plastic hinging within the column. Both the positive and negative moment flexural capacity of the superstructure should be calculated based on strain compatibility or a moment-curvature analysis. Articles 8.10, 8.11, and 8.12 of the Seismic Guide Specifications give guidance to the effective width of the superstructure that should be used in assessing the capacity in both the longitudinal and transverse directions for both integral and nonintegral superstructures.

The Seismic Guide Specifications do not directly specify the shear capacity of a capacity-protected member. Instead, reference is made to the Bridge Design Specifications. The superstructure shear capacity should be calculated in accordance with article 5.8.3.3 of the Bridge Design Specifications for concrete superstructures.

Shear Blocks

Shear blocks serve to transfer the transverse superstructure inertial loads to the abutments through shear. The capacity of all shear blocks should be calculated during design. For this example, the capacity of the shear blocks has not been calculated. Instead, it has been assumed

the blocks have sufficient strength. The calculation should be made in accordance with article 5.8.4 of the Bridge Design Specifications.

Prestressed Girder Anchorage

To create a fully integral bent cap system, the prestressed concrete girders must be anchored sufficiently to the cast-in-place diaphragm to resist column overstrength forces. Of primary concern is the development of positive moment capacity at the cap beam; negative moment strength will be provided by the steel in the topping slab.

The WSDOT BDM provides a procedure to determine the number of prestressing strands to extend from the girder into the cast-in-place diaphragm using the equation shown in figure 36. The calculated number of strands must be greater than four and not exceed one-half of the total number of straight strands.

$$N_{ps} = (M_{sei}K - M_{SIDL}) \frac{1}{0.9\phi A_{ps}f_{py}d}$$

Figure 36. Equation. Number of extended strands.

The moment due to the overstrength moment capacity of the column, and the associated overstrength shear, is defined in figure 37.

$$M_{sei} = \frac{2}{3}(M_{po} + V_{po}D_{s1})$$

Figure 37. Equation. Moment due to column plastic overstrength forces.

In figure 37:

V_{po} = Column overstrength shear

D_{s1} = Height of the lower precast cap beam

M_{SIDL} = Moment due to superimposed dead load over the effective width

K = Span moment distribution factor (maximum of K_1 and K_2 from figure 38)

A_{ps} = Area of each extended strand

F_{py} = Yield strength of prestressing strand (per Bridge Design Specifications)

d = Distance from the top of deck slab to center of gravity of extended strands

ϕ = Flexural resistance factor (taken as 1.0)

The moment due to the overstrength demand from column hinging within the effective width is calculated as follows:

$$M_{sei} = \frac{2}{3}(M_{po} + V_{po}D_{s1}) = \frac{2}{3}(3,528 \text{ kip-ft} + (344 \text{ kip})(36 \text{ in.})) = 3,040 \text{ kip-ft}$$

Because the bridge has equal span lengths, the span distribution factor can be taken to be:

$$K = K_1 = K_2 = 0.5$$

If the moment due to superimposed dead load is taken to be zero (which is conservative), then the number of bottom strands that are required to be extended into the cast-in-place diaphragm is calculated as shown below, using 0.6-inch-diameter 270 ksi seven-wire strands with an effective depth of 39.25 inches.

$$N_{ps} = (M_{sei}K - M_{SIDL}) \frac{1}{0.9\phi A_{ps} f_{py} d} = \frac{(3,040 \text{ kip-ft})(0.5) - 0}{0.9(1.0)(0.217 \text{ in}^2)(243 \text{ ksi})(39.25 \text{ inches})}$$

$$N_{ps} = 9.79 \text{ strands}$$

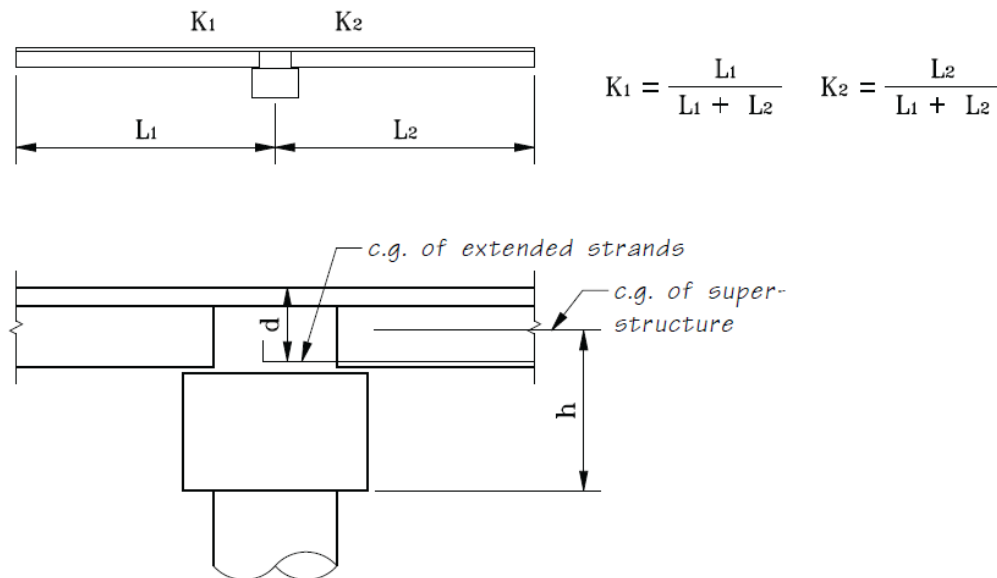


Figure 38. Diagram. Extended strand design (from WSDOT BDM).⁽³⁾

Because there are two girders within the effective width, each girder needs at least five extended strands. For the final design, six strands were extended into the cast-in-place diaphragm. These extended strands must be detailed such that they achieve full continuity between girders of adjacent spans, which guarantees a robust load path for the tensile horizontal joint forces. WSDOT released a design memorandum (08-2012) which outlines three possible methods (in order of preference) for developing this continuity. They are reproduced here verbatim:

Method 1:

Direct extended strands overlapping shall be used at intermediate piers without any angle point due to horizontal curvature and for any crossbeam width. This is the preferred method of achieving extended strand continuity. Congestion of reinforcement and girder setting constructability shall be considered when large numbers of extended strands are required. In these cases, strand ties may be used in conjunction with extended strands.

Method 2:

Strand ties shall be used at intermediate piers with a girder angle point due to horizontal curvature where extended strands are not parallel and would cross during girder placement. Crossbeam widths shall be greater than or equal to 6 ft measured along the skew. It is preferable that strand ties be used for all extended strands, however if the region becomes too congested for rebar placement and concrete consolidation, additional forces may be carried by crossbeam ties up to a maximum limit as specified in equation (1) below.

Method 3:

For crossbeams with widths less than 6 feet and a girder angle point due to horizontal curvature, strand ties shall be used if a minimum of 8 inches of lap can be provided between the extended strand and strand tie. In this case the strand ties shall be considered fully effective. For cases where less than 8 inches of lap is provided, the effectiveness of the strand tie shall be reduced proportional to the reduction in lap. All additional forces not taken by strand ties must be carried by crossbeam ties up to the maximum limit as specified in equation (1) below. If this limit is exceeded, the geometry of the width of the crossbeam shall be increased to provide sufficient lap for the strand ties.

The area of transverse ties considered effective for strand ties development in lower crossbeam shall not exceed:

$$A_s = \frac{1}{2} \frac{A_{ps} f_{py} n_s}{f_{ye}} \quad (1)$$

Where:

- A_{ps} = Area of strand ties, in²
- n_s = Number of extended strands that are spliced with strand and crossbeam ties
- f_{py} = Yield strength of extended strands, ksi
- f_{ye} = Expected yield strength of reinforcement, ksi

Two-thirds of A_s shall be placed directly below the girder and the remaining of A_s shall be placed outside the bottom flange width. The size of strand ties shall be the same as the extended strands, and shall be placed at the same level and proximity of the extended strands.

Cap Beam

To understand the loading to which the cap beam will be subjected, it is necessary to examine how the bridge will be constructed. The lower precast cap beam will be fabricated off-site in two pieces; after the columns have been constructed, the lower cap beam segments will be set onto the columns and grouted into place. The two segments will then be made continuous via a cast-

in-place closure pour within the central span. The precast end panels will then be installed and the precast girder set onto the cap beam one span at a time. The bottom 1 foot 2 inches of the intermediate pier diaphragm (stage 2 of the cap beam), the abutment end diaphragms, and the intermediate diaphragms will be poured to secure the girders in place. The bridge deck topping will then be cast. Finally, the top portion of the intermediate pier diaphragm (cap beam) will be cast along with the pedestrian barriers.

This construction sequence allows the girders to be simply supported under dead load, which will reduce the cracking in the bridge deck due to negative moment at the piers. The specific loading cases that must be considered will be addressed in turn.

The lower cap beam was cast in two separate pieces and spliced together using a cast-in-place closure pour in the central span. The closure location will typically be placed at about one-third of the span so that it is roughly at the inflection point of a continuous span. Considerations need to be made for shipping, handling, and construction loading on the lower cap beam, which resulted in the cap beam being concentrically prestressed to prevent cracking of the section during handling.

Once the lower cap beam is made continuous and grouted to the columns, the section must be strong enough to resist the dead load of the upper cap beam, the girders, the topping slab, the diaphragms, and the barriers. Additionally, the torsion applied by girders being set on one span only should be considered along with the construction live load.

The fully composite cap beam and integral girder connection should then be checked for flexure, shear, and torsion, as would typically be done, to provide adequate strength for the forces within the completed structure. Care should be taken to account for the locked-in dead load stresses within the lower cap beam.

Considering the loading, the lower cap beam was designed with the following:

- **Thirty-six 0.6-inch-diameter prestressing strands** to control the tensile stresses in the lower cap beam due to shipping and handling loads, and live load negative moments.
- **Fifteen No. 11 bars** in the bottom layer to resist the lower cap beam dead and construction loads (eight bars), and the live loads and plastic hinging forces within the final condition (seven bars).
- **Fourteen No. 11 bars** in the top layer of the lower cap beam to resist the negative moments over the center columns due to dead and construction loading.
- **Eight No. 11 bars** under the bottom mat of the deck to resist the plastic hinging forces of the exterior columns.

The Seismic Guide Specifications do not directly specify the shear capacity of a capacity-protected member. Instead, reference is made to the Bridge Design Specifications. The cap beam shear capacity should be calculated in accordance with article 5.8.3.3 of the Bridge Design Specifications.

The shear reinforcement in the lower cap beam was No. 6 four leg closed stirrups at 6 inches on center (o.c.), with additional single leg No. 7 stirrups at 6 inches o.c. extending from the lower cap beam into the upper cast-in-place diaphragm.

Column-to-Cap Beam Connection

The column-to-cap beam joint must be designed to transmit the plastic overstrength forces produced by the column into the superstructure. This calculation must be done in accordance with article 8.13 of the Seismic Guide Specifications.

Due to the precast dropped cap beam and the cast-in-place stage 2 diaphragm, special care is needed to anchor the column longitudinal bars in the cap beam to adequately transfer column forces into the joint and into the superstructure. In this particular design, the column bars were anchored into oversized corrugated metal ducts using high-strength grout, and they were extended beyond the precast cap as far into the cast-in-place diaphragm as possible.

Once the column plastic hinging forces are transferred into the stage 2 diaphragm there must be a load path into the superstructure. As the negative moment strength in the girders is provided by the steel in the topping slab, a mechanism must be provided to enable the forces to round the corner between the vertical column bars and the horizontal topping slab bars. This is accomplished by the stirrups within the girders, which hook above the topping steel, and the J-bars provided due to the bridge skew. It is recommended that J-bars be provided even if a skew does not exist.

Figure 39 shows a section through the cap beam and the amplified flexural demand imposed on the interface between the precast cap beam and the cast-in-place diaphragm due to plastic hinging within the column under longitudinal seismic excitation. (Note that the girder stirrups and J-bars are not shown in figure 39.) The interface between stages 1 and 2 should be capacity-protected; therefore, additional reinforcement crossing the interface is needed in the form of cap beam stirrups.

Despite the amplified demand on the interface, the load will spread transversely along the length of the cap beam. This spreading results in an effective width of the superstructure, which is taken as B_{eff} and is shown in figure 40. Two-thirds of the amplified flexural demand is assumed to be resisted by B_{eff} while the remaining one-third is resisted by the superstructure on either side of the effective width. If B_{eff} from adjacent columns overlaps, a uniform distribution of moments should be assumed along the span of cap beam between columns.

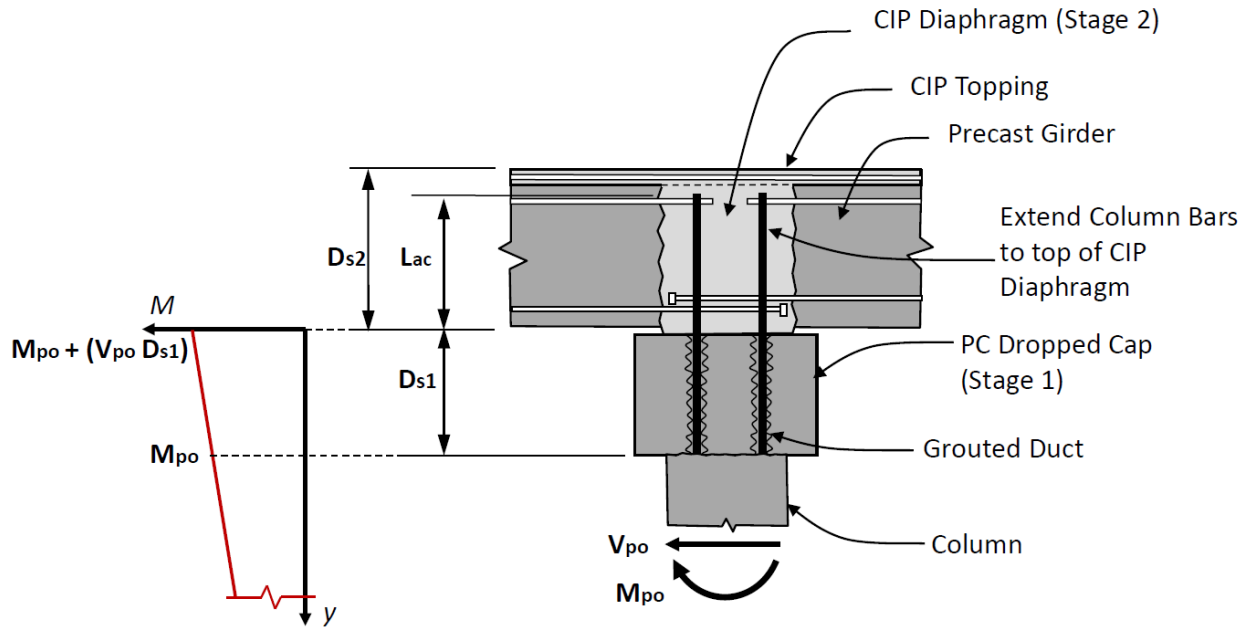


Figure 39. Diagram. Longitudinal force transfer at the cap beam interface.

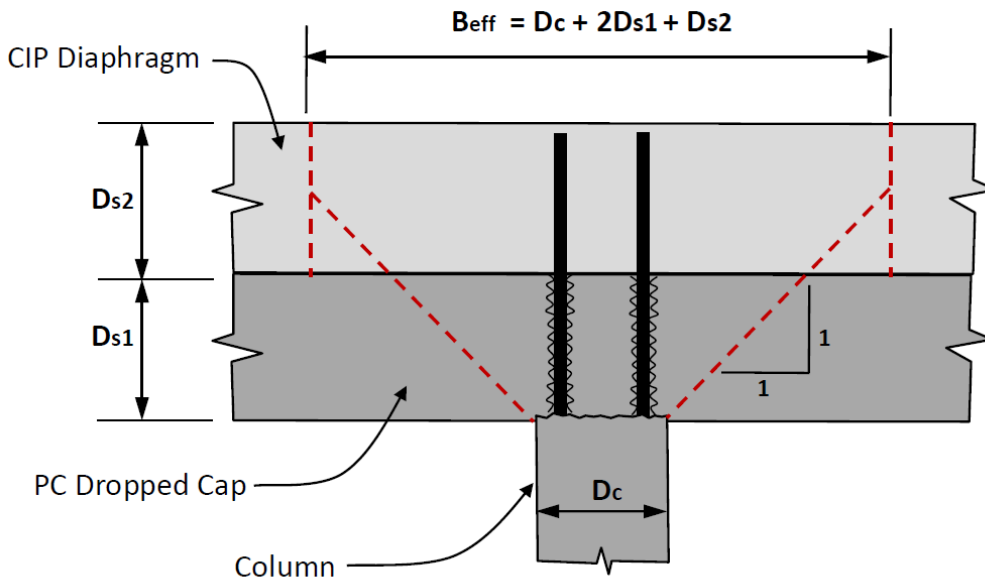


Figure 40. Diagram. Longitudinal effective superstructure width.

If large-diameter column reinforcing bars are used, full development can be difficult to achieve above the interface between the precast cap beam and the cast-in-place diaphragm. In this case, the available strength of the column bars is reduced to roughly the proportion of the development length provided. For this bridge, eight No. 14 bars ran from the column into the precast dropped cap and into the cast-in-place diaphragm. Due to the small depth of the prestressed concrete girders, the column bars only extended 34 inches above the interface. Article 8.8.4 of the Seismic

Guide Specifications stipulates that the anchorage length of column longitudinal bars is calculated using equation 8.8.4-1, shown here in figure 41.

$$l_{ac} \geq \frac{0.79d_{bl}f_{ye}}{\sqrt{f'_c}}$$

Figure 41. Equation. Column longitudinal bar anchorage length.

For this design example:

$$l_{ac} \geq \frac{0.79(1.693 \text{ inch})(68 \text{ ksi})}{\sqrt{4 \text{ ksi}}} = 45.5 \text{ inches}$$

Assuming constant bond stress, the available axial bar stress at incipient bond failure is taken to be as shown in figure 42.

$$f_{s,avail} = \frac{l_{prov}}{l_{ac}} f_{ye}$$

Figure 42. Equation. Available axial bar stress.

For this design example:

$$f_{s,avail} = \frac{34 \text{ inches}}{45.5 \text{ inches}} (68 \text{ ksi}) = 50.8 \text{ ksi}$$

Where:

$$l_{prov} = \text{Provided development length (inches)}$$

The strength at the interface must be evaluated to ensure full capacity protection and a robust load path of column overstrength forces into the superstructure. Two checks are therefore required: (1) sufficient area of steel crossing the interface and (2) an adequately sized and reinforced joint region. These will be addressed in turn.

Equation 8.13.2-8 in the Seismic Guide Specifications can be used to determine the column tensile force in lieu of a moment-curvature analysis or mechanics-based calculation, but in some cases it can yield very conservative results, especially for an integral bent loaded longitudinally. The following section highlights the use of a mechanics-based approach verified using a moment-curvature analysis. The demand on the interface due to column plastic hinging is determined through the free body diagram shown in figure 43, where the only unknown is the net tensile force resultant (T_c).

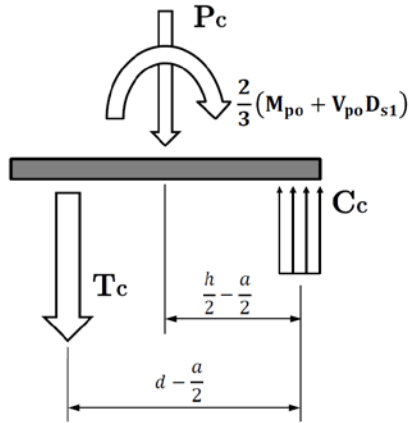


Figure 43. Diagram. Interface mechanics.

Equilibrium leads to the equation in figure 44:

$$T_c = \frac{\frac{2}{3}(M_{po} + V_{po}D_{sl}) - P_c\left(\frac{h}{2} - \frac{a}{2}\right)}{d - \left(\frac{a}{2}\right)}$$

Figure 44. Equation. Tensile resultant force.

Where:

M_{po} = Column overstrength moment

V_{po} = Column overstrength shear

D_{sl} = Height of the lower precast cap beam

P_c = Column axial load at the interface

h = Total depth of the cap beam

a = Depth of the compression block

d = Effective depth to the net tension force

To calculate the net tension resultant in the bars crossing the interface, the location of the resultant force needs to be approximated along with the depth of the compression block. Assuming that the column bars have not slipped, the depth to the force resultant (d) can be taken as the centroid of the steel crossing the interface neglecting any bars that are close to the neutral axis of the section. Figure 45 shows the geometry of the interface.

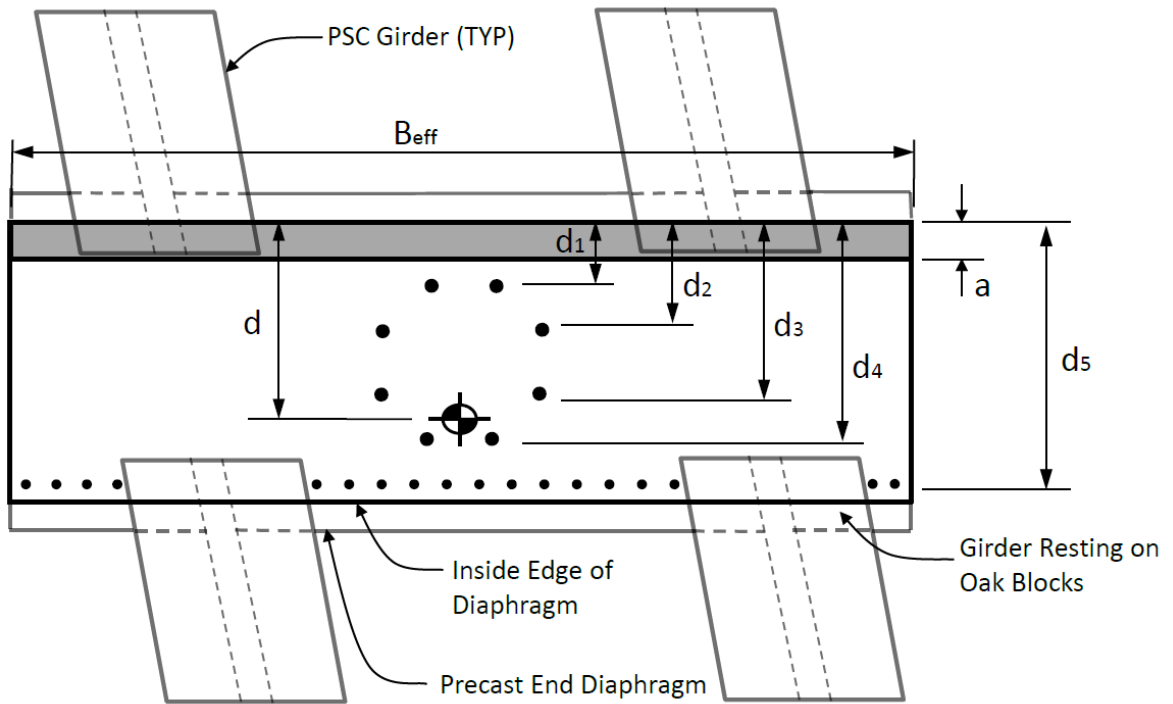


Figure 45. Diagram. Interface geometry.

For this bridge, the layering of the steel crossing the interface is given in table 24.

Table 24. Interface geometry.

Layer Number	Area of Steel	Depth to Layer	Comments
1	4.5 in ²	14.1 inches	Two No. 14 column bars
2	4.5 in ²	25.2 inches	Two No. 14 column bars
3	4.5 in ²	40.9 inches	Two No. 14 column bars
4	4.5 in ²	52.0 inches	Two No. 14 column bars
5	10.8 in ²	62.3 inches	Eighteen No. 7 stirrups

The analytical section is defined as the area enclosed by the precast end diaphragms. This limit was chosen because the girders are set on oak blocks, reducing the effective depth of the interface section.

Using the equation shown in figure 46, it is determined that the net tensile reaction is located 44 inches away from the compressive face. It should be noted again that this assumes the column reinforcing bars have not slipped; this assumption depends on the geometry and the loading of the dropped cap beam, but it should result in a conservative approximation because it shifts the location of T_c towards the neutral axis, thereby increasing the magnitude of T_c .

$$d = \frac{\sum_i^n A_i d_i}{\sum_i^n A_i}$$

Figure 46. Equation. Distance to the tensile force resultant.

In figure 46:

A_i = Area of steel in layer i

d_i = Distance to layer i from the compression face

The final assumption is the depth of the compression block (a). Here it can be assumed that the compression block is roughly $0.1d$, which is a common assumption in the initial design of singly reinforced non-prestressed sections. The net tensile force reaction can then be approximated as shown below:

$$T_c = \frac{\frac{2}{3} \left(3,528 \text{ kip-ft} \left(\frac{12 \text{ in.}}{\text{in.}} \right) + (344 \text{ kip})(36 \text{ in.}) \right) - 800 \text{ kip} \left(\frac{66 \text{ in.}}{2} - \frac{4.4 \text{ in.}}{2} \right)}{44 \text{ in.} - \left(\frac{4.4 \text{ in.}}{2} \right)} = 283 \text{ kip}$$

The capacity of the reinforcement crossing the interface is calculated as follows:

$$T_n = A_s f_{ye} = (8)(2.25 \text{ in}^2)(50.8 \text{ ksi}) + (18)(0.6 \text{ in}^2)(68 \text{ ksi}) = 1,648.8 \text{ kip}$$

Clearly, the interface has enough strength to resist the overstrength demands from column hinging.

The value of the net tensile force can also be determined using a moment-curvature analysis of the section, the results of which are shown in figures 47 and 48, where it can be seen that the assumption that the column bars do not slip is valid, and the approximate calculated value of T_c (283 kips) is close to the more refined calculation based on the moment-curvature analysis (253 kips). It is plain to see that the interface has adequate strength and is capacity-protected.

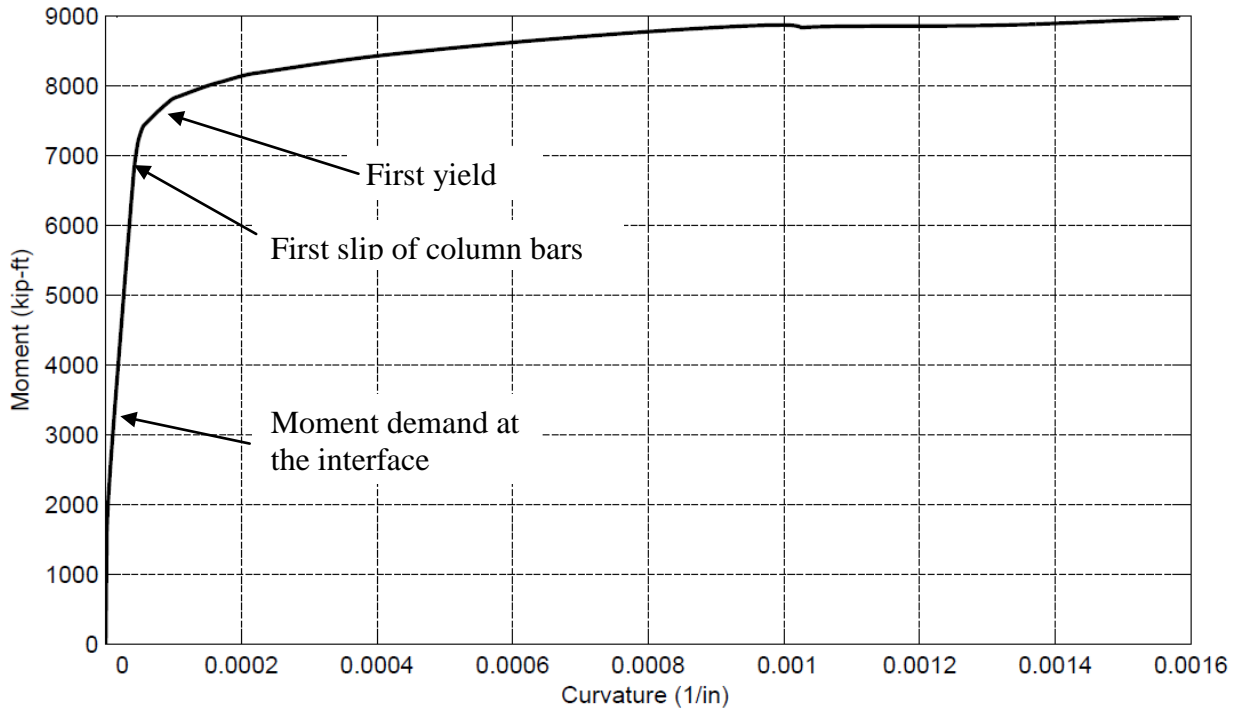


Figure 47. Graph. Interface moment-curvature response.

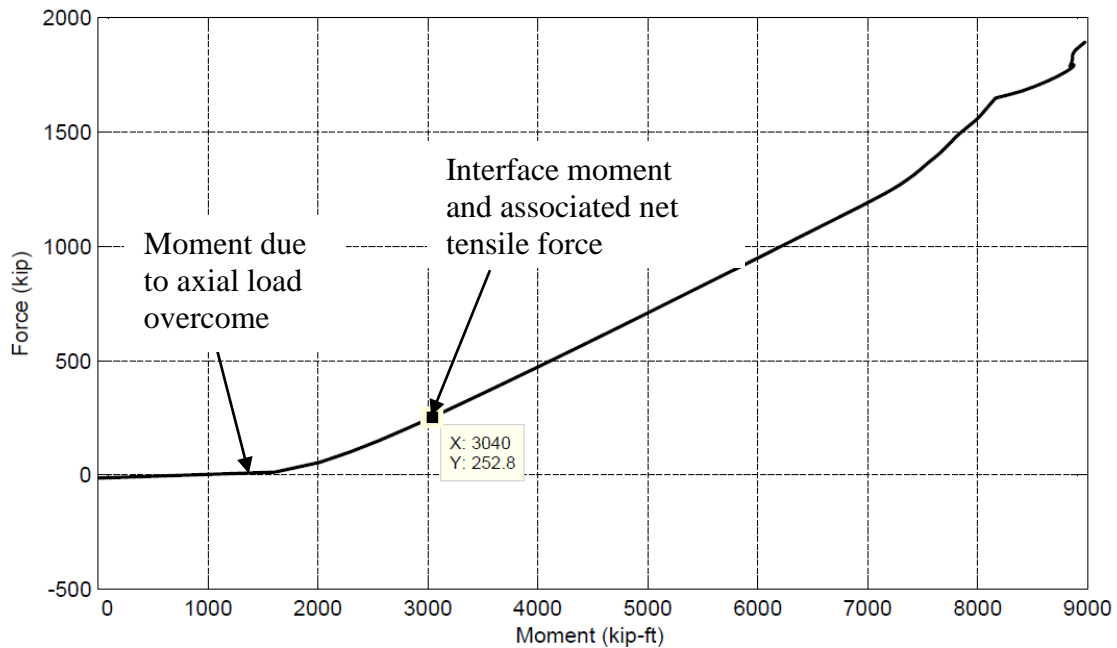


Figure 48. Graph. Interface net tensile force.

As the cap beam is integrally connected to the superstructure in both the longitudinal and transverse directions, the joint shear must be checked for each load direction. Under transverse seismic loading, the joint dimensions are defined as shown in figures 49 through 51, while the joint for the longitudinal loading is shown in figures 52 through 54. The precast girders have been omitted from the figures for clarity, but they would run orthogonally or skewed to the axis of the cast-in-place diaphragm and precast dropped cap.

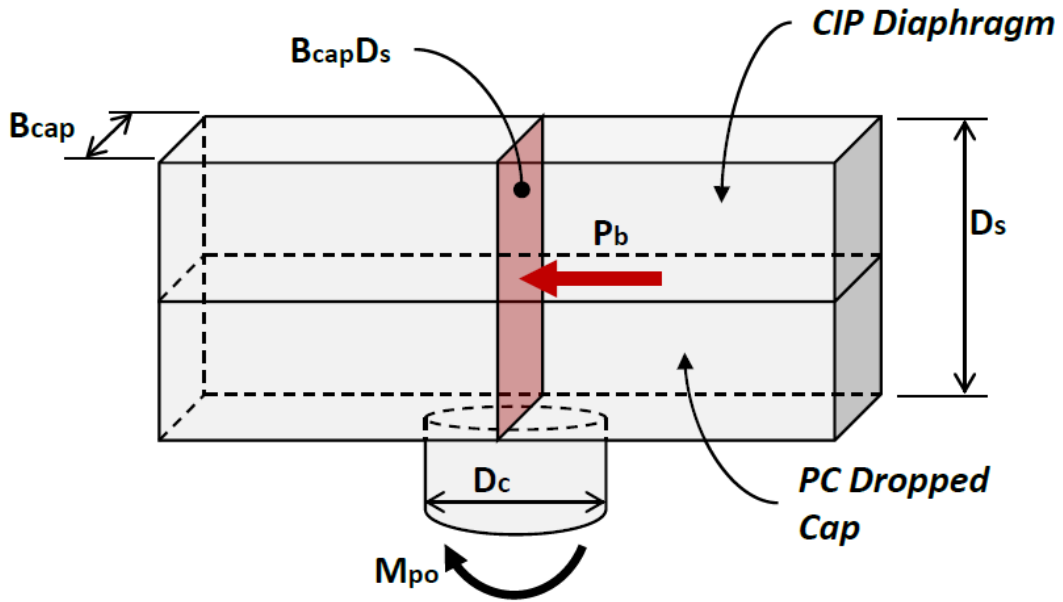


Figure 49. Diagram. Transverse loading—horizontal normal joint stress.

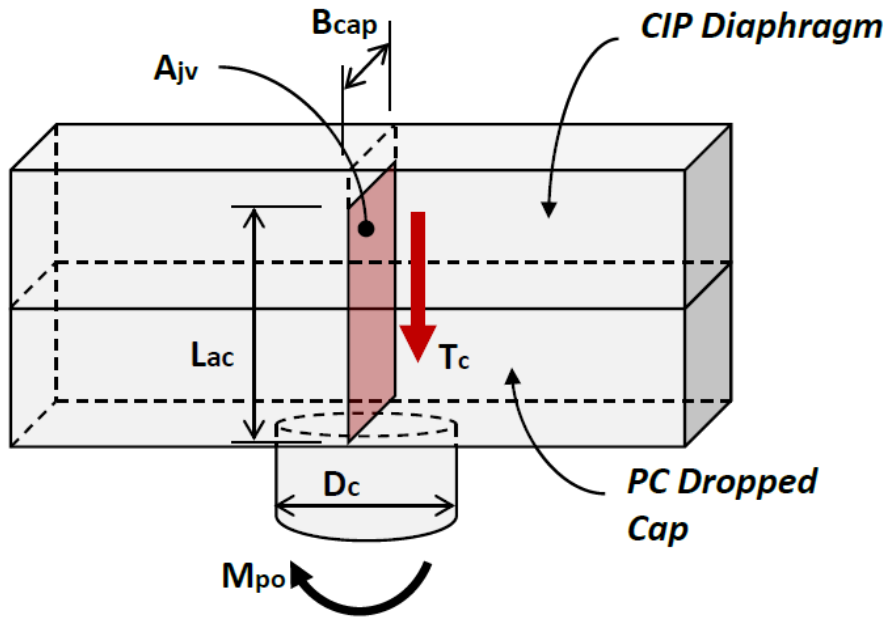


Figure 50. Diagram. Transverse loading—vertical joint shear stress.

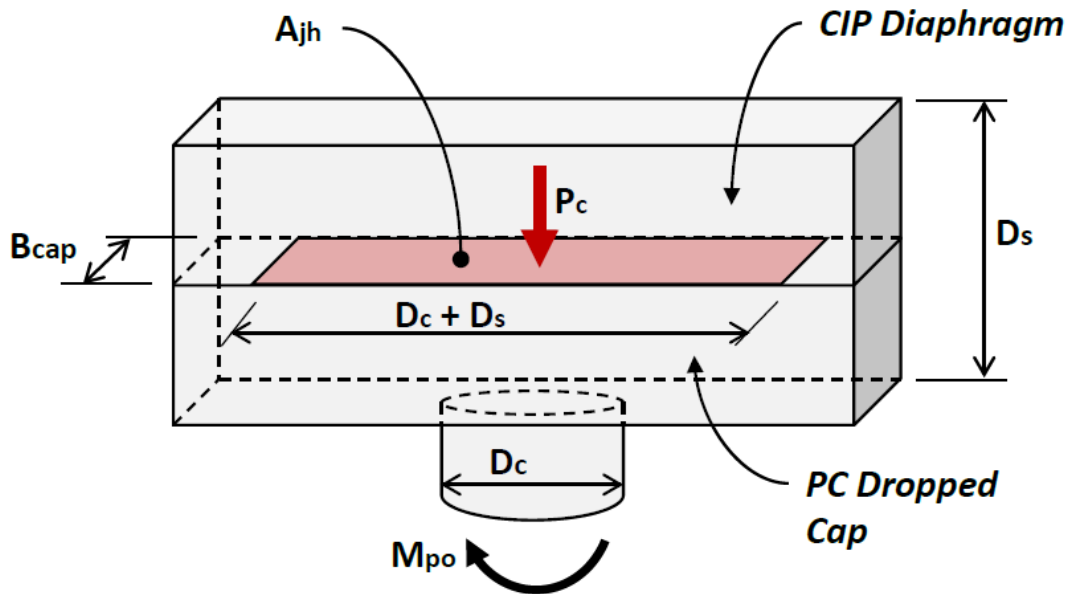


Figure 51. Diagram. Transverse loading—vertical normal joint stress.

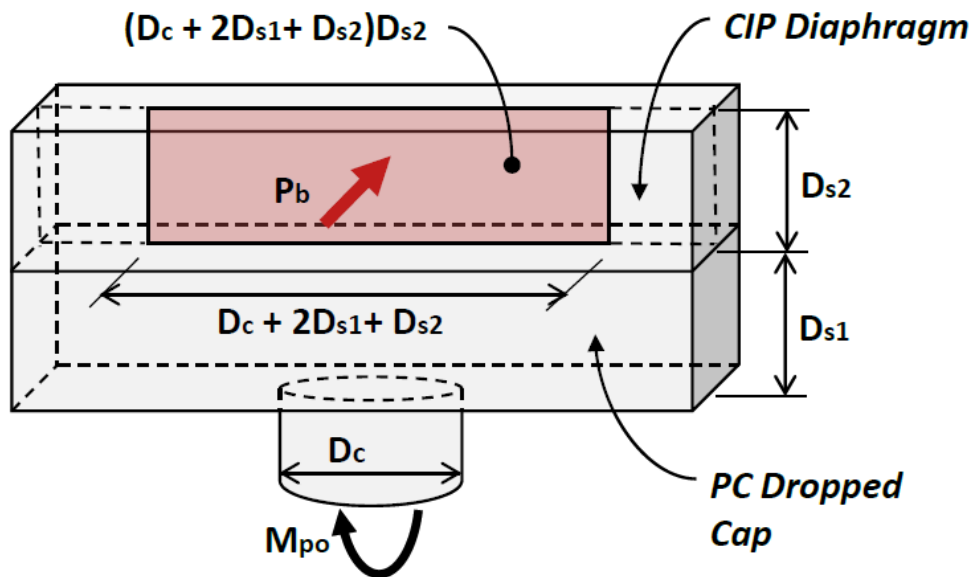


Figure 52. Diagram. Longitudinal loading—horizontal normal joint stress.

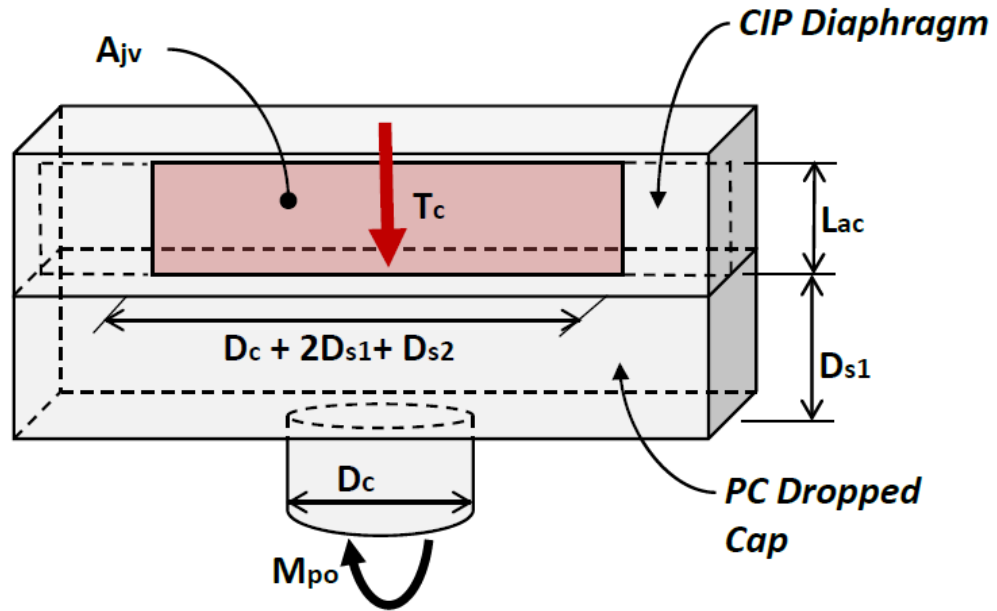


Figure 53. Diagram. Longitudinal loading—vertical joint shear stress.

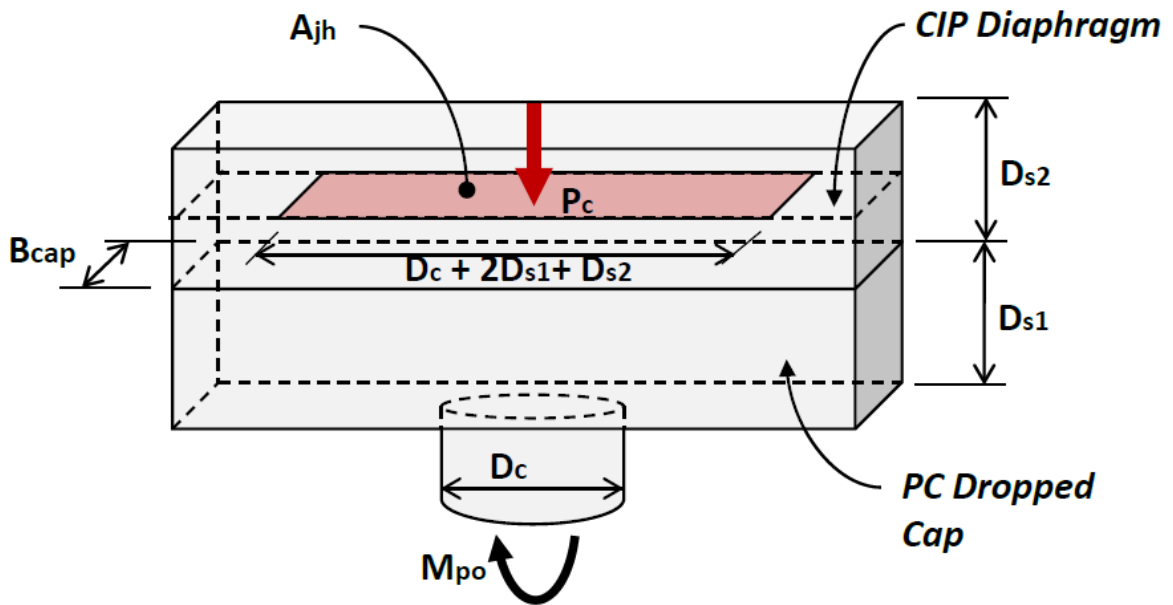


Figure 54. Diagram. Longitudinal loading—vertical normal joint stress.

As can be seen, the joint can be substantially reduced in size for the longitudinal seismic loading depending on the structural geometry. This can potentially cause difficulty in proportioning the joint; furthermore, this is an area of high congestion, due to multiple lap splices, anchorage of column longitudinal bars, spiral around column bars, and supplemental joint reinforcing if cracked conditions exist.

After the dimensions of the joint regions are defined, the joint shear calculations can be made using the methods in article 8.13.2 of the Seismic Guide Specifications, as described in the following subsections.

Joint Shear in the Transverse Direction

First, determine the column tensile force associated with plastic hinging using the equation in figure 55.

$$T_c = 0.7A_{st}f_{ye}$$

Figure 55. Equation. Column tensile force associated with plastic hinging.

$$T_c = 0.7(8)(2.25 \text{ in}^2)(68 \text{ ksi}) = 857 \text{ kip}$$

Then calculate the vertical joint shear stress using the equation in figure 56.

$$v_{jv} = \frac{T_c}{A_{jv}} = \frac{T_c}{L_{ac}B_{cap}}$$

Figure 56. Equation. Vertical joint shear stress from loading in the transverse direction.

$$v_{jv} = \frac{857 \text{ kip}}{(72 \text{ in.})(66 \text{ in.})} = 0.180 \text{ ksi}$$

Calculate the vertical normal joint stress. Due to overturning of the pier, the vertical normal stress should be calculated for the lowest and highest observed axial loads, using the equations in figures 57 and 58. The lowest will control the principal tension, while the highest will control the principal compression.

$$f_{v,min} = \frac{P_{c,min}}{A_{jh}} = \frac{P_{c,min}}{B_{cap}(D_c + D_s)}$$

Figure 57. Equation. Minimum vertical joint shear stress from loading in the transverse direction.

$$f_{v,min} = \frac{391 \text{ kip}}{(66 \text{ in.})(48 \text{ in.} + 80 \text{ in.})} = 0.046 \text{ ksi}$$

$$f_{v,max} = \frac{P_{c,max}}{A_{jh}} = \frac{P_{c,max}}{B_{cap}(D_c + D_s)}$$

Figure 58. Equation. Maximum vertical joint shear stress from loading in the transverse direction.

$$f_{v,max} = \frac{956 \text{ kip}}{(66 \text{ in.})(48 \text{ in.} + 80 \text{ in.})} = 0.113 \text{ ksi}$$

Next, calculate the horizontal normal joint stress using the equation in figure 59. In this bridge, the pier the stage 1 dropped cap beam is prestressed while the stage 2 diaphragm is normal reinforced concrete. The prestressing force is used to increase the principal compression while it is neglected in the calculation of the principal tension. The prestress force is assumed to be

spread over the entire joint region, not just the precast first stage, which is conservative, as it lowers the effective compression on the joint.

$$f_{h,PSC} = \frac{P_b}{B_{cap}D_{s1}}$$

Figure 59. Equation. Horizontal normal joint stress from loading in the transverse direction.

$$f_{h,PSC} = \frac{1,411 \text{ kip}}{(78 \text{ in.})(36 \text{ in.})} = 0.503 \text{ ksi}$$

$$f_{h,CIP} = 0 \text{ ksi}$$

The principal stresses are calculated by combining the applied loading that will result in the highest tensile and compressive stresses, as shown below. This gives a conservative stress for each case.

$$p_t = \left| \left(\frac{f_{h,CIP} + f_{v,min}}{2} \right) - \sqrt{\left(\frac{f_{h,CIP} - f_{v,min}}{2} \right)^2 + v_{jv}^2} \right|$$

Figure 60. Equation. Principal tension from loading in the transverse direction.

$$p_t = \left| \left(\frac{0 \text{ ksi} + 0.046 \text{ ksi}}{2} \right) - \sqrt{\left(\frac{0 \text{ ksi} - 0.046 \text{ ksi}}{2} \right)^2 + (0.180 \text{ ksi})^2} \right| = 0.158 \text{ ksi}$$

$$p_c = \left| \left(\frac{f_{h,PSC} + f_{v,max}}{2} \right) + \sqrt{\left(\frac{f_{h,PSC} - f_{v,max}}{2} \right)^2 + v_{jv}^2} \right|$$

Figure 61. Equation. Principal compression from loading in the transverse direction.

$$p_c = \left| \left(\frac{0.503 \text{ ksi} + 0.113 \text{ ksi}}{2} \right) + \sqrt{\left(\frac{0.503 \text{ ksi} - 0.113 \text{ ksi}}{2} \right)^2 + (0.180 \text{ ksi})^2} \right| = 0.573 \text{ ksi}$$

The principal stresses will then be checked against the cracking and ultimate limit stresses to determine if the joint is adequately proportioned and reinforced.

$$P_{c,ult} = 0.25f'_c$$

Figure 62. Equation. Ultimate principal compression.

$$P_{c,ult} = 0.25(4 \text{ ksi}) = 1.0 \text{ ksi} \geq p_c \rightarrow \text{OK!}$$

$$P_{t,ult} = 0.38 \sqrt{f'_c}$$

Figure 63. Equation. Ultimate principal tension.

$$P_{t,ult} = 0.38 \sqrt{4 \text{ ksi}} = 0.76 \text{ ksi} \geq p_t \rightarrow \text{OK!}$$

$$P_{t,crack} = 0.11 \sqrt{f'_c}$$

Figure 64. Equation. Cracking principal tension.

$$P_{t,crack} = 0.11 \sqrt{4 \text{ ksi}} = 0.22 \text{ ksi} \geq p_t \rightarrow \text{Joint Uncracked!}$$

It can be seen that the joint is adequately proportioned and is uncracked; thus the minimum joint shear reinforcement from article 8.13.3 of the Seismic Guide Specifications applies. However for this example, the prescriptive reinforcement for a cracked joint is shown below for illustrative purposes. These calculations are provided solely to illustrate the process for a cracked joint.

Spiral with the minimum volumetric reinforcing ratio shall be placed around the embedded column bars within the joint, as calculated from figure 65.

$$\rho_s \geq 0.4 \frac{A_{st}}{L_{ac}^2}$$

Figure 65. Equation. Minimum volumetric reinforcing ratio for cracked joints.

$$\rho_s \geq 0.4 \frac{(8)(2.25 \text{ in}^2)}{(72 \text{ in.})^2} = 0.0014$$

Assuming a No. 5 spiral, the required maximum pitch is calculated using the equation in figure 66.

$$s \leq \frac{4A_{sp}}{D_{core}\rho_s}$$

Figure 66. Equation. Spacing of transverse reinforcement.

$$s \leq \frac{4(0.31 \text{ in}^2)}{(44 \text{ in.})(0.0014)} = 20 \text{ in.}$$

The final design utilized a No. 5 spiral with a 4-inch pitch, which is sufficient. Welded circular hoops at the same spacing could be used to reduce congestion.

Vertical stirrups or ties shall be placed within one column diameter from the centerline of the column with a total area equal to A_s^{jv} on each side of the column in the direction of loading, where A_s^{jv} is calculated as shown in figure 67.

$$A_s^{jv} \geq 0.20A_{st}$$

Figure 67. Equation. Area of joint vertical reinforcement.

$$A_s^{jv} \geq 0.20(8)(2.25 \text{ in}^2) = 3.6 \text{ in}^2$$

The final design used No. 7 stirrups at 5 ½ inches o.c. along the length of the cap beam. These stirrups were omitted at the location of the prestressed concrete girder to prevent severe congestion. This resulted in six No. 7 bars within one column diameter from each side of the column centerline (total area = 3.6 in²), which is sufficient.

Horizontal stirrups or ties shall be placed around the vertical stirrups or ties in two or more intermediate layers spaced vertically no more than 18 inches apart and within one column diameter from the column centerline. The area of horizontal reinforcement is determined using the equation in figure 68.

$$A_s^{jh} \geq 0.10A_{st}$$

Figure 68. Equation. Area of joint horizontal reinforcement.

$$A_s^{jh} \geq 0.10(8)(2.25 \text{ in}^2) = 1.8 \text{ in}^2$$

Horizontal stirrups were placed in five layers at 12 inches o.c. vertically and 22 inches apart along the length of the cap beam. This resulted in 18 No. 4 horizontal ties (total area = 3.6 in²), which is sufficient.

Horizontal side reinforcement shall be placed near the side face of the cap at no more than 12 inch spacing. The area of side reinforcement is determined using the equation in figure 68.

$$A_s^{sf} \geq \max \begin{cases} 0.1A_{cap}^{top} \\ 0.1A_{cap}^{bot} \end{cases}$$

Figure 69. Equation. Area of joint side reinforcement.

$$A_s^{sf} \geq \max \begin{cases} 0.1(8)(1.56 \text{ in}^2) \\ 0.1(16)(1.56 \text{ in}^2) \end{cases} = \max \begin{cases} 1.25 \text{ in}^2 \\ 2.5 \text{ in}^2 \end{cases} = 2.5 \text{ in}^2$$

Side reinforcement was placed as five layers of continuous No. 6 bars at 12 inches o.c. vertically on each face (total area = 4.4 in²), which is sufficient.

Finally, because the bridge is at a skew of more than 20 degrees, J-bars are necessary with the following minimum area of steel.

$$A_s^{j-bar} \geq 0.08A_{st}$$

Figure 70. Equation. Area of J-bar reinforcement.

$$A_s^{j-bar} \geq 0.08(8)(2.25 \text{ in}^2) = 1.44 \text{ in}^2$$

The final design used eight No. 4 J-bars over each column in two rows of four bars (total area = 1.6 in²), which is sufficient. For the placement of the additional joint reinforcement, see figures 8.13.4.1.2a-1 through 8.13.4.1.2a-3 in the Seismic Guide Specifications.

Joint Shear in the Longitudinal Direction

In the case of loading in the longitudinal direction, the column tensile force term in the joint shear stress equations is taken as the force calculated across the interface between the upper and the lower stages of the cap beam. This force likely will be different from the column tensile force for loading in the transverse direction.

$$T_c = 283 \text{ kips}$$

First, calculate the vertical joint shear stress using the equation in figure 71.

$$v_{jv} = \frac{T_c}{A_{jv}} = \frac{T_c}{L_{ac}(D_c + 2D_{s1} + D_{s2})}$$

Figure 71. Equation. Vertical joint shear stress from loading in the longitudinal direction.

$$v_{jv} = \frac{283 \text{ kip}}{(33 \text{ in.})(48 \text{ in.} + 2(39 \text{ in.}) + 41 \text{ in.})} = 0.051 \text{ ksi}$$

Next, calculate the horizontal normal joint stress. Again, the lowest and highest axial loads should be used to determine the worst case principal stresses, as shown in figures 72 and 73.

$$f_{v,min} = \frac{P_{c,min}}{A_{jh}} = \frac{P_{c,min}}{B_{cap}(D_c + 2D_{s1} + D_{s2})}$$

Figure 72. Equation. Minimum vertical joint shear stress from loading in the longitudinal direction.

$$f_{v,min} = \frac{594 \text{ kip}}{(66 \text{ in.})(48 \text{ in.} + 2(39 \text{ in.}) + 41 \text{ in.})} = 0.0016 \text{ ksi}$$

$$f_{v,max} = \frac{P_{c,max}}{A_{jh}} = \frac{P_{c,max}}{B_{cap}(D_c + 2D_{s1} + D_{s2})}$$

Figure 73. Equation. Maximum vertical joint shear stress from loading in the longitudinal direction.

$$f_{v,max} = \frac{878 \text{ kip}}{(66 \text{ in.})(48 \text{ in.} + 2(39 \text{ in.}) + 41 \text{ in.})} = 0.0024 \text{ ksi}$$

Calculate the horizontal normal joint stress using the equation in figure 74.

$$f_h = \frac{P_b}{D_{s2}(D_c + 2D_{s1} + D_{s2})}$$

Figure 74. Equation. Horizontal normal joint stress from loading in the longitudinal direction.

$$f_h = 0 \text{ ksi}$$

Then calculate the principal stresses using the equations in figures 75 and 76.

$$p_t = \left| \left(\frac{f_{h,CIP} + f_{v,min}}{2} \right) - \sqrt{\left(\frac{f_{h,CIP} - f_{v,min}}{2} \right)^2 + v_{jv}^2} \right|$$

Figure 75. Equation. Principal tension from loading in the longitudinal direction.

$$p_t = \left| \left(\frac{0 \text{ ksi} + 0.0016 \text{ ksi}}{2} \right) - \sqrt{\left(\frac{0 \text{ ksi} - 0.0016 \text{ ksi}}{2} \right)^2 + (0.051 \text{ ksi})^2} \right| = 0.05 \text{ ksi}$$

$$p_c = \left| \left(\frac{f_{h,PSC} + f_{v,max}}{2} \right) + \sqrt{\left(\frac{f_{h,PSC} - f_{v,max}}{2} \right)^2 + v_{jv}^2} \right|$$

Figure 76. Equation. Principal compression from loading in the longitudinal direction.

$$p_c = \left| \left(\frac{0.0024 \text{ ksi} + 0.0016 \text{ ksi}}{2} \right) + \sqrt{\left(\frac{0.0024 \text{ ksi} - 0.0016 \text{ ksi}}{2} \right)^2 + (0.051 \text{ ksi})^2} \right| = 0.053 \text{ ksi}$$

The principal stresses will then be checked against the cracking and ultimate limit stresses to determine if the joint is adequately proportioned and reinforced, using the equations in figures 77 through 79.

$$P_{c,ult} = 0.25 f'_c$$

Figure 77. Equation. Ultimate principal compression.

$$P_{c,ult} = 0.25(4 \text{ ksi}) = 1.0 \text{ ksi} \geq p_c \rightarrow \text{OK!}$$

$$P_{t,ult} = 0.38 \sqrt{f'_c}$$

Figure 78. Equation. Ultimate principal tension.

$$P_{t,ult} = 0.38 \sqrt{4 \text{ ksi}} = 0.76 \text{ ksi} \geq p_t \rightarrow \text{OK!}$$

$$P_{t,crack} = 0.11 \sqrt{f'_c}$$

Figure 79. Equation. Cracking principal tension.

$$P_{t,crack} = 0.11 \sqrt{4 \text{ ksi}} = 0.22 \text{ ksi} \geq p_t \rightarrow \text{Joint Uncracked!}$$

Because the joint is well proportioned and uncracked, only the minimum spiral around the column bars is required (see figure 80).

$$\rho_s \geq \frac{0.11 \sqrt{f'_c}}{f_{ye}}$$

Figure 80. Equation. Minimum volumetric reinforcing ratio for uncracked joints.

$$\rho_s \geq \frac{0.11 \sqrt{4 \text{ ksi}}}{68 \text{ ksi}} = 0.0032$$

Assuming a No. 5 spiral, the required maximum pitch is calculated as shown in figure 81.

$$s \leq \frac{4A_{sp}}{D_{core}\rho_s}$$

Figure 81. Equation. Spacing of transverse reinforcement.

$$s \leq \frac{4(0.31 \text{ in}^2)}{(44 \text{ in.})(0.0032)} = 8.7 \text{ in.}$$

The final design used a No. 5 spiral with a 4-inch pitch, which is sufficient. Welded circular hoops at the same spacing could be used to reduce congestion. For the placement of the additional joint reinforcement see figures 8.13.4.1.2a-1 through 8.13.4.1.2a-3 in the Seismic Guide Specifications.

Column Splices

To make a fully precast column system viable, it may be necessary to build the column using multiple precast segments, in which case one or more mid-height column splices are needed. Splices should be located outside of the plastic hinge region as determined by article 4.11.7 of the Seismic Guide Specifications. The plastic hinge region is defined as the larger of the following:

- 1.5 times the column diameter.
- The region of the column where the moment demand exceeds 75 percent of the maximum plastic moment.
- The analytical plastic hinge length.

These provisions result in the following lengths:

- 1.5 (48 inches) = 72 inches.
- 44.8 inches.
- 37.5 inches.

Therefore, the splice can be located no closer than 72 inches to the cap beam soffit or the top of the footing. Both the shear capacity across the segment interface and the ability of the splice to develop the necessary moment capacity must be checked.

For this particular bridge, three segments were used; see figures 82 through 84. This was done to demonstrate how to build column joints. The columns would have otherwise been single pieces. It can be seen that both the top and the bottom segments have No. 14 bars extending into the middle segment, where they are developed into grout filled tubes. The middle segment then uses two bundled No. 10 bars to lap with each No. 14 bar to maintain continuity in the reinforcement. It is important that the No. 14 bars are fully developed into the middle segment (to provide the shear friction resistance) and the No. 10 bars have sufficient lap length to transfer necessary column flexural forces.

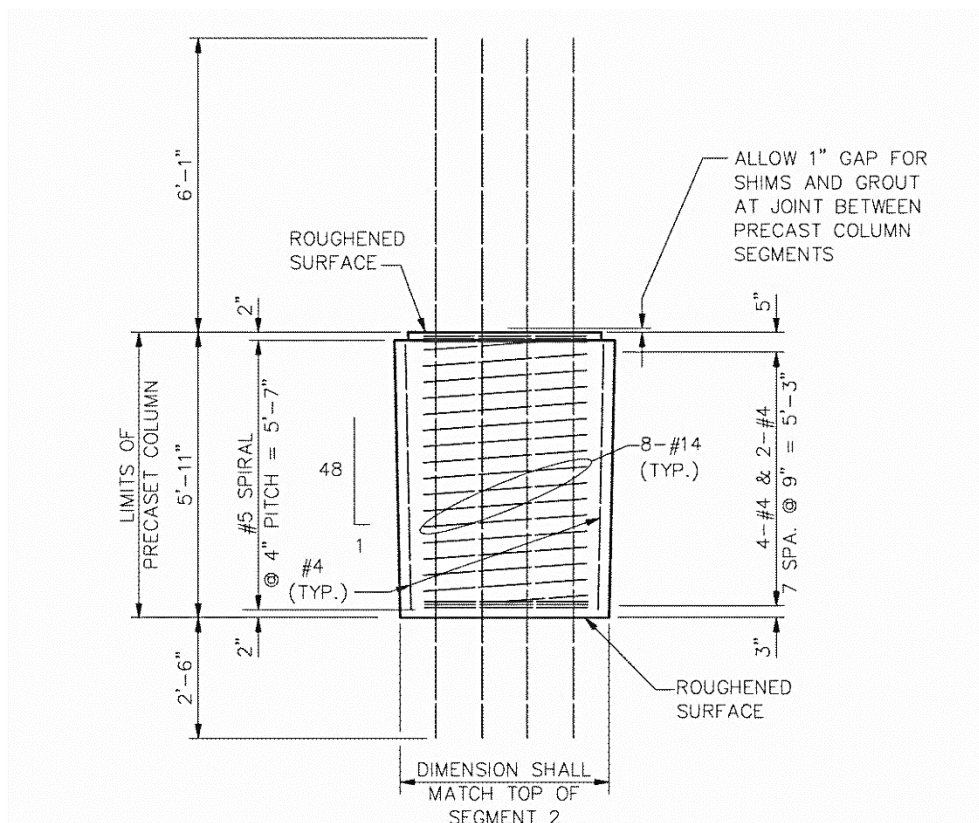


Figure 82. Diagram. Top of column segment.

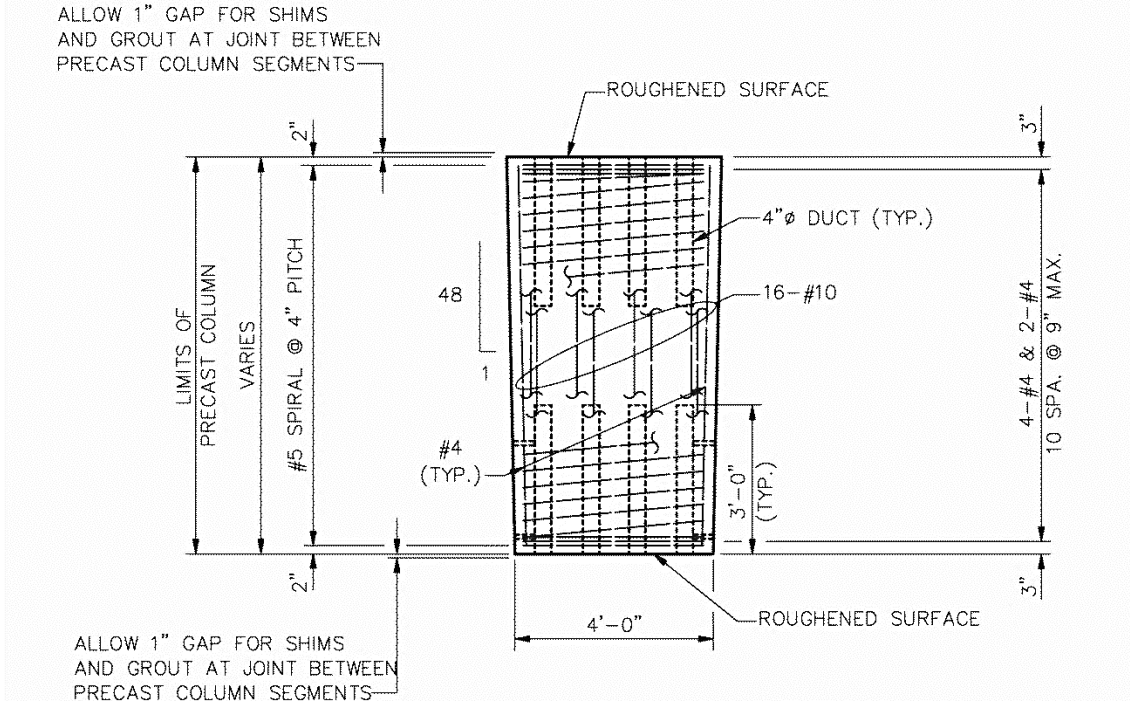


Figure 83. Diagram. Middle column segment.

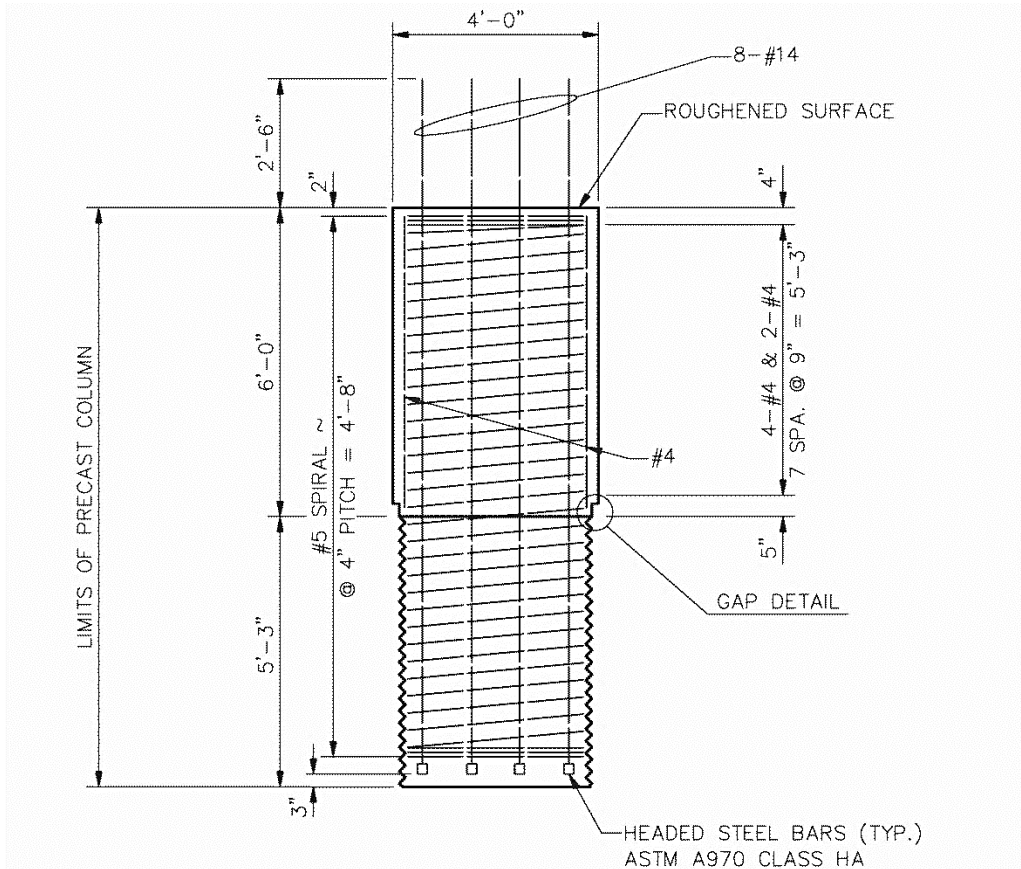


Figure 84. Diagram. Bottom of column segment.

The first check discussed is the shear friction strength check across the roughened surface interface between the precast column segment and the grout closure. The shear friction strength, per article 5.8.4 of the Bridge Design Specifications, is as shown in figures 85 through 87.

$$V_{ni} = cA_{cv} + \mu(A_{vf}f_y + P_c)$$

Figure 85. Equation. Nominal shear friction capacity.

$$V_{ni} \leq K_1 f'_c A_{cv}$$

Figure 86. Equation. First upper limit of shear friction capacity.

$$V_{ni} \leq K_2 A_{cv}$$

Figure 87. Equation. Second upper limit of shear friction capacity.

To account for cyclic loading effects and the potential for significant cracking, use $c = 0$, $\mu = 0.6$, $K_1 = 0.2$, $K_2 = 0.8$, $\phi = 0.9$, and $f_y = 60$ ksi. The minimum axial load on the column under a transverse seismic event is 391 kips, while the maximum column shear due to plastic hinging forces is equal to 361 kips (note these demands do occur concurrently on the same column, but a check that uses them will be conservative for all columns).

$$V_{ni} = 0 + 0.6 \left((8)(2.25 \text{ in}^2)(60 \text{ ksi}) + 391 \text{ kip} \right) = 882.6 \text{ kip}$$

$$V_{ni} \leq 0.2(4 \text{ ksi})(48 \text{ in.})(48 \text{ in.}) = 1,843 \text{ kip}$$

$$V_{ni} \leq (0.8 \text{ ksi})(48 \text{ in.})(48 \text{ in.}) = 1,843 \text{ kip}$$

$$\phi V_{ni} = 0.9(882.6 \text{ kip}) = 794.3 \text{ kip} \geq V_u = 361 \text{ kip} \rightarrow \text{OK!}$$

The column splice will therefore have sufficient shear strength to handle plastic hinging shear forces in all columns. The column splice will also need to resist any flexural forces across the interface.

Research at the University of Washington has shown that large-diameter bars grouted into metal ducts can be developed in a short distance, as determined with the equation in figure 88.⁽⁸⁾

$$l_{ac} = \frac{0.67 d_{bl} f_{ye}}{\sqrt{f'_g}}$$

Figure 88. Equation. Development length for a bar grouted into a metal duct.

Therefore, the No. 14 bars ($d_{bl} = 1.693$ inches) must be extended a minimum of 27.3 inches into the metal duct (using $f_{ye} = 68$ ksi and $f'_g = 8$ ksi). Testing has demonstrated that the ducts can adequately transfer force to smaller bars outside the ducts when the splice length of the smaller bars is used to design the bar-to-duct lap length.

To determine the lap splice length for the No. 10 bars the flexural demand on the splices must be determined. This is done using the moment diagram shown in figure 89 for the seismic overstrength case (plastic hinging at the top and bottom of the column). The demands from non-seismic load combinations should be checked to verify they do not control the splice strength.

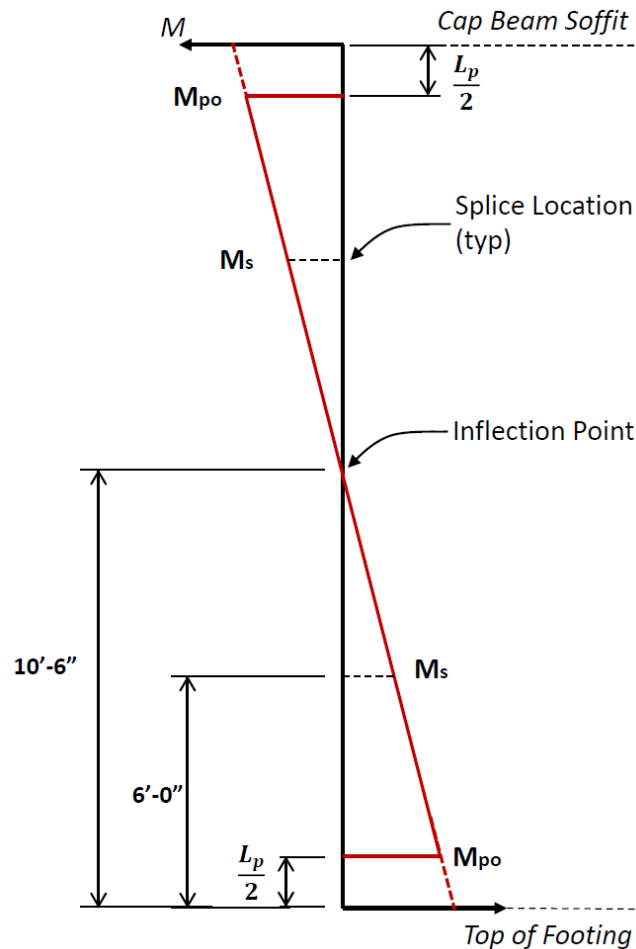


Figure 89. Diagram. Flexural demands on column splices.

If the plastic overstrength moment (M_{po}) is taken at $L_p/2$ away from the top and bottom of the column, then the flexural demand at the splice is found by similar triangles. For the geometry of the column and the location of the splices, this results in a demand of $0.5M_{po}$, as the splice is almost exactly halfway between the location of M_{po} and the inflection point. Once the flexural demand on the splice is determined, the required splice length for the No. 10 bars can be calculated using the Bridge Design Specifications provisions of article 5.11.5. The base development length of a No. 10 bar is calculated as shown in figure 90.

$$l_{db} = \frac{1.25A_b f_{ye}}{\sqrt{f'_c}}$$

Figure 90. Equation. Base development length.

$$l_{db} = \frac{1.25(1.27 \text{ in.}^2)(68 \text{ ksi})}{\sqrt{4 \text{ ksi}}} = 54.0 \text{ in.}$$

The AASHTO provisions allow this length to be reduced by several applicable modification factors. First, the splice length can be reduced by a factor of 0.75 if the reinforcement is confined by spiral with a bar size larger than 0.25 inches in diameter, as long as the spiral is at a 4-inch pitch or less. Additionally, the development length can be multiplied by the ratio of the area of steel provided to the area of steel required at the location of the splice. Since the flexural demand at the splice is 50 percent of the overstrength demand, the area required at the splice will be equal to 50 percent of the area of the No. 14 bar. The area of steel provided will then be equal to the area of the two No. 10 bars in the lap splice. This results in the following modification factor:

$$\frac{A_{s,Required}}{A_{s,Provided}} = \frac{0.5(2.25 \text{ in.}^2)}{2(1.27 \text{ in.}^2)} = 0.443$$

Therefore, the development length for the No. 10 bars in the middle section is:

$$l_d = 0.75(0.443)(54.0 \text{ in.}) = 17.9 \text{ in.}$$

The splice length depends on the stress in the bars at the splice and the number of bars being spliced at one location. As shown above, the area of steel provided is greater than 2 times the area of steel required ($1/0.443 = 2.257$), and all of the bars will be spliced at one location. Therefore, the splice is categorized as a Class B splice, and as such the splice length is $1.3l_d$.

$$l_s = 1.3l_d = 1.3(17.9 \text{ in.}) = 23.3 \text{ in.}$$

The overall splice length is controlled by the development of the No. 14 bars in the metal ducts at a minimum length of 27.1 inches. For the final design, the No. 14 bars were extended 30 inches from the top and the bottom segments. With the 1-inch-thick grout joint between segments, this provided a length of 29 inches grouted into the metal ducts, which exceeds the minimum required for both the development of the No. 14 bar and the splice of the No. 10 bars.

Spread Footing

The spread footings must be proportioned and designed to resist overturning, sliding, flexure, and shear per article 6.3 of the Seismic Guide Specifications. For this example, the typical cast-in-place spread footing design calculations are not shown, as the emphasis of this example is to show the special considerations needed for a fully precast bridge system.

To allow for the socket connection where the precast column runs through the entire footing depth, the flexural reinforcement that would lie under the column if the bars were uniformly spaced must be moved and bundled on either side of the column. This is shown schematically in figure 91. The slab reinforcement should be bundled as close to the column as is reasonably possible to ensure an efficient force transfer.

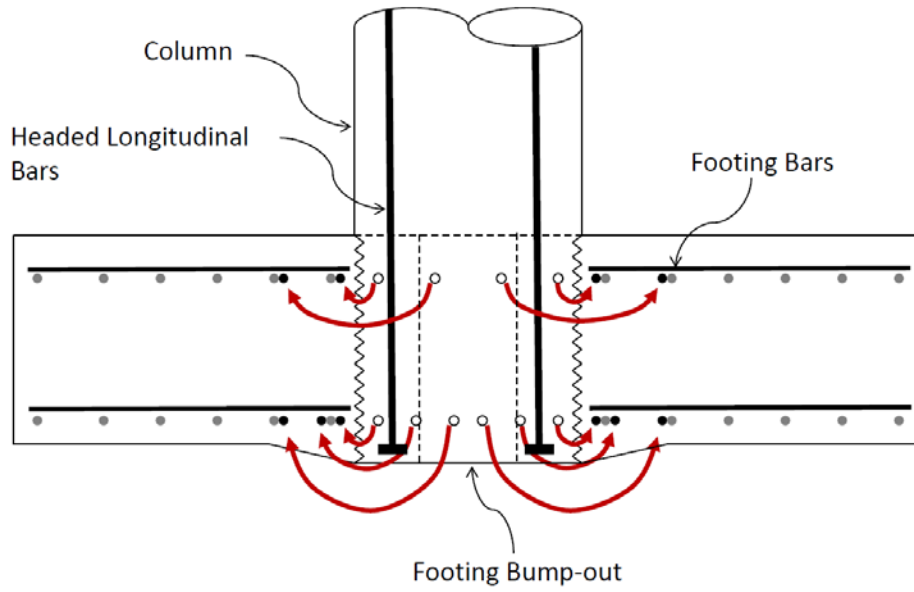


Figure 91. Diagram. Adjustment of footing flexural reinforcement.

Additionally, experimental testing has shown that the column longitudinal reinforcement must be anchored below the bottom mat of the slab flexural reinforcement to develop a robust strut-and-tie mechanism, as shown in figure 92. This may require a bump-out on the bottom of the footing under the column to maintain clear cover to the headed bars. The strut-and-tie model for a conventional cast-in-place column is shown in figure 93 to show the difficulty in forming a well-defined node within the joint due to the turned out column bars. The compression strut within the joint has to develop tangentially against the bend of the column bar.

Experimental research has shown that shallow footings ($\sim 0.5D_{column}$) can be susceptible to punching shear failures due to combined shear and moment transfer around the column perimeter. Therefore, care should be taken in determining the footing depth.

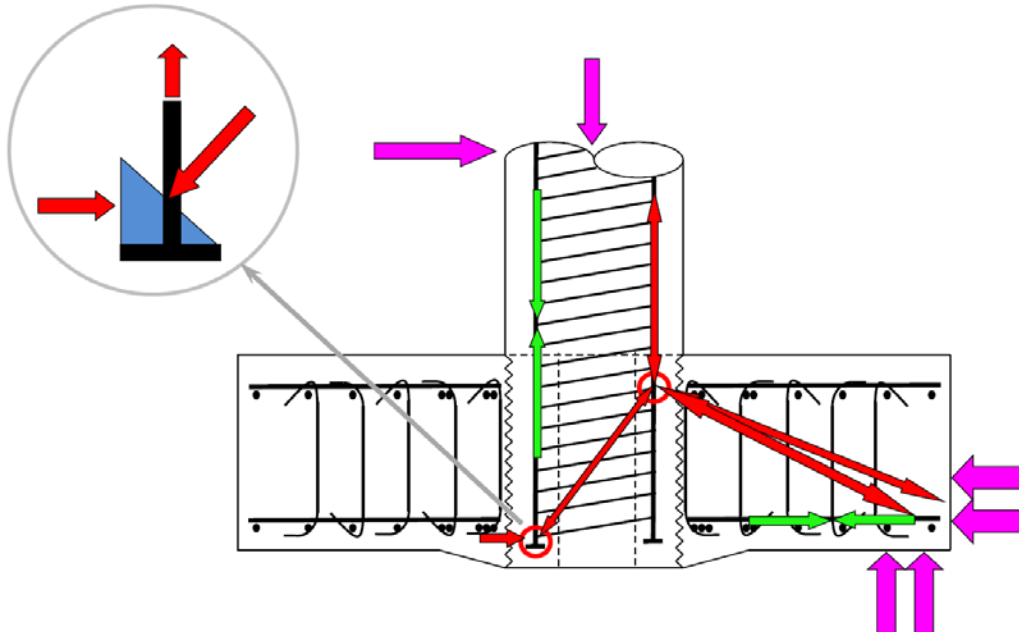


Figure 92. Diagram. Precast column strut-and-tie mechanism.

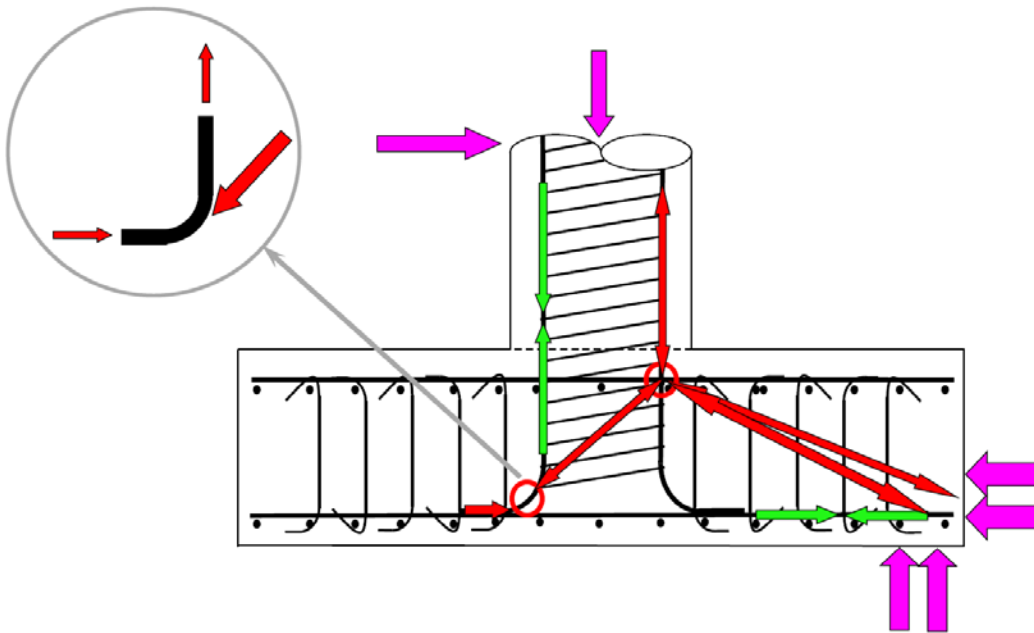


Figure 93. Diagram. Conventional cast-in-place column strut-and-tie mechanism.

Socket Connection of Column to Spread Footing

The column-to-footing joint must be designed to transmit the plastic overstrength forces produced by the column (i.e., ductile member), similar to the column-to-cap beam connection. This calculation must be done in accordance with article 6.4.5 of the Seismic Guide Specifications.

Of particular concern with the socket type connection for a precast column is whether the column will punch through the footing under axial load. It is imperative that a positive force transfer mechanism be provided at the interface between the precast column embed and the cast-in-place footing. For consistency with the tests in which the detail was developed, the embedded portion of the column should be of an octagonal cross-section with 1-inch saw-tooth roughening. If the saw-tooth is formed using timber strips, a polygonal, rather than a circular, shape may facilitate construction. An octagonal section was used in the tests; however, a circular section would be acceptable if the saw-tooth can be formed in it.

The force transfer will be designed using shear friction principles, and as such, additional reinforcement around the perimeter of the embedded column is required to provide a normal clamping force (see figure 94). The maximum factored column axial load should be used for this calculation.

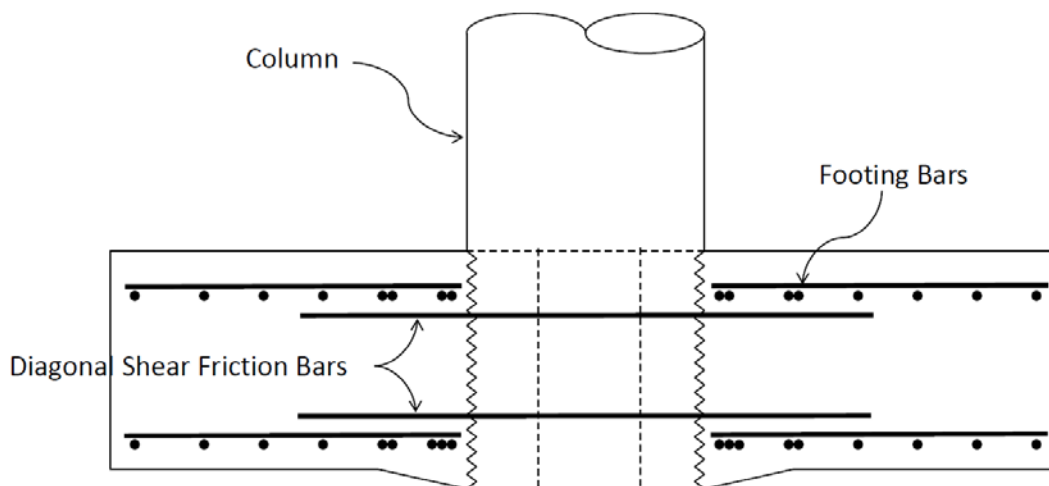


Figure 94. Diagram. Additional shear friction reinforcement.

The resistance to shear across the cold joint between the column and the footing concrete is determined using the equation in figure 95, from article 5.8.4 of the Bridge Design Specifications.

$$V_{ni} = cA_{cv} + \mu(A_{vf}f_y + P_c)$$

Figure 95. Equation. Nominal shear friction capacity.

In the design of the shear friction steel, to remain conservative it should be assumed that there is no concrete contribution, and no cohesion—the only resistance is provided by the clamping force of the additional steel. Therefore, $c = 0$ and $P_c = 0$, and if there is any shrinkage cracking, a conservative interface strength is provided. The resulting capacity of the interface is determined using the equation in figure 96.

$$\phi V_{ni} = \phi \mu A_{vf} f_y$$

Figure 96. Equation. Capacity of column-to-footing interface.

Using normal weight concrete cast against a clean, intentionally roughened surface, use $\mu = 1.0$, $\phi = 0.9$, $f_y = 60$ ksi, and rearranging terms with $V_u = \phi V_{ni}$.

$$A_{vf} \geq \frac{V_u}{\phi \mu f_y}$$

Figure 97. Equation. Minimum required shear friction reinforcement.

$$A_{vf} \geq \frac{1,752 \text{ kips}}{0.9(1.0)(60 \text{ ksi})} = 32.4 \text{ in.}^2$$

Assuming that there are two shear planes orthogonal to each other in plan, the required area of steel per direction is 16.2 in.^2 , which results in 13 No. 10 bars per direction. In the final design, 16 No. 10 bars were used top and bottom. The bars should be fully developed by the time they reach the edge of the column. The layout of the bars in plan is shown in figure 98. The diagonal bars are the shear friction reinforcement and consist of 4 No. 10 bars on each side of the column in both the top and bottom mats (32 bars total). The bundled bars can be seen, along with the footing joint shear reinforcement.

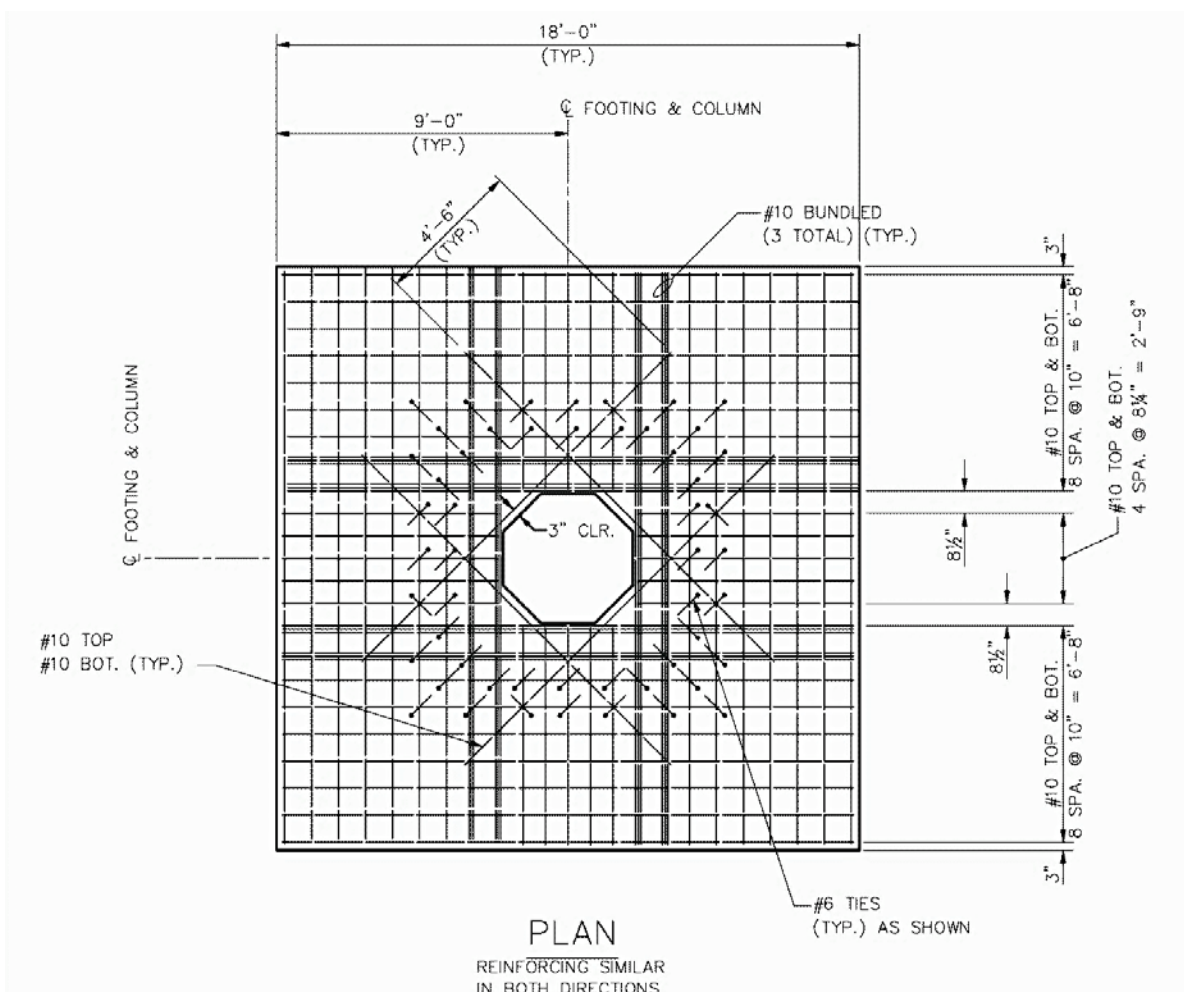


Figure 98. Diagram. Footing reinforcement plan.

CHAPTER 7. CONSTRUCTABILITY CONSIDERATIONS

For a fully precast bridge bent system to be feasible and cost-effective, careful planning is required, particularly in regards to the fabrication, shipping, erection, constructability, and fit-up of the precast segments. This chapter discusses some of the primary considerations.

SIZE OF PRECAST ELEMENTS

The size of precast elements will be based on several important considerations, including the size, weight, and strength restrictions for transportation and erection.

Transportation Dimension and Weight Restrictions

Some precast elements, such as columns and cap beams, are quite stocky and, as such, concentrate a large portion of their weight onto relatively few truck axles. Consideration must be given to the legal axle weight limits, the dimensions of the precast component, and the distribution of components weight along the length of a truck bed.

Crane Pick Weight

Depending on any site access restrictions, the size of precast elements may be limited by the type and size of cranes that can fit on the site. In some cases, such as for the bridge used in this design example, where the intermediate bent falls within the center median of a busy roadway below, multiple cranes may be needed to lift, maneuver, and erect the precast elements.

Transportation and Erection Loading

When precast elements are transported and erected, various types of loading may be imposed upon them, all of which must be accounted for in the design using stress checks so that the components do not crack during transportation and erection. If elements are predicted to crack under construction loading, several options exist. Alternative lifting point configurations can be investigated, the size of the precast element can be reduced, or the element can be prestressed to reduce the net tensile stresses within the concrete. For the bridge used in this design example, the cap beam segments were concentrically prestressed to prevent cracking when the segments were lifted into place. Temporary strands may also be used in certain situations to post-tension (unbonded) the precast element before shipping and erection, then removed after the element has been placed. Typically, the ducts are filled with grout after the temporary strands have been removed.

CAP BEAM FIT-UP WITH COLUMNS

To accommodate the cross-slope or super-elevation of a bridge with precast elements, several cap beam, girder, and roadway slab configurations can be used:

- **Level cap beam top and bottom surfaces** – This configuration requires that the bridge cross-slope and super-elevation is generated using pads on top of the girders or a variable thickness roadway slab. The bottom of the cap beam will be parallel to the top of the

upper column segment and may have a uniform depth recess to accept the top of the column to provide enhanced corrosion resistance.

- **Sloped cap beam top surface, level bottom surface** – This configuration requires that the cross-slope and super-elevation is generated with a uniform thickness roadway slab on top of the varying elevations of the top of the girders. Again, the bottom of the cap beam will be parallel to the top of the upper column segment and may have a uniform depth recess to accept the top of the column to provide enhanced corrosion resistance.
- **Sloped cap beam top and bottom surfaces** – This configuration requires that the bridge cross-slope and super-elevation is generated with a uniform thickness roadway slab on top of the varying elevations of the top of the girders. The bottom of the cap beam will need to be notched or recessed to generate a parallel surface between the bottom of the cap beam and the top of the upper column segment. The depth of this recess will depend on the magnitude of the cap beam slope and the desired corrosion protection.

The third option was used for the bridge in this design example.

CONSTRUCTION SEQUENCE

While the construction sequence has been addressed at various points throughout this design example, it is outlined here for the sake of completeness.

1. Excavate for footing and install forms.
2. Place leveling pad at bottom of the footing excavation and set first segment of column (as seen in figure 99).
3. Place footing reinforcing and cast footing concrete.
4. Remove forms and backfill around the excavation.
5. Place and shim middle column segments.
6. Place and shim top column segments.
7. Install column bracing.
8. Place and shim precast bent cap segments (as seen in figure 100).
9. Install grout forms and seal.
10. Pump grout and close grout tubes (all column segment joints and the column-to-cap beam connection were grouted in one operation).
11. Remove grout forms and inspect grout in joint and grout tubes.
12. Repair unfilled grout tubes and patch back grout tubes.
13. Place precast girders on oak blocks one span at a time.
14. Install girder bracing if necessary.
15. Complete welded ties between girders.
16. Join flange shear keys and grout intermediate diaphragms.
17. Place slab reinforcement and cast roadway slab concrete.
18. Cast pier diaphragm concrete 10 days after slab casting. Note that each deck-bulb tee was fitted with a precast end wall, with the intent of reducing the amount of formwork needed.
19. Cast traffic barrier and sidewalk.



Figure 99. Photos. Construction sequence for placement of first precast column segment.



Figure 100. Photo. Precast cap beam placement.

CHAPTER 8. CLOSING REMARKS

The design checks show the bridge passes all capacity-to-demand requirements of the Seismic Guide Specifications. Analysis has shown that the displacement requirements have been easily satisfied with C/D ratios of 2.86 for the longitudinal direction and 4.06 for the transverse direction. This indicates that there is a possibility for additional refinement to the bridge design.

Refinement may include an adjustment to the number or size of the longitudinal and/or lateral confining reinforcement in the columns. The possibility of this reduction assumes there is additional steel in the members beyond the minimum requirements for non-seismic analysis of flexure and shear.

From the viewpoint of seismic loading, it may be possible to reduce the number of columns in each bent. The reduced stiffness would be expected to increase the displacement of the piers, but the displacement capacity is high and may tolerate the additional demand. However, the vertical load design, and particularly that of the precast cap beam, would have to be checked.

Overall, the design is satisfactory.

ACKNOWLEDGEMENTS

The authors would like to acknowledge that this design example is based on the National Highway Institutes Course No. 130093 Design Example No. 1 (Publication No. FHWA-NHI-04-160). Some sections are reproduced here verbatim, others have been modified to remain congruent with the Highways for LIFE demonstration project, and many sections have been added to specifically address the Highways for LIFE fully precast bent system for seismic regions and the associated design criteria that have been developed herein.

REFERENCES

1. AASHTO. (2011). *AASHTO Guide Specifications for LRFD Seismic Bridge Design* (Second ed.). Washington, DC: American Association of State Highway and Transportation Officials.
2. AASHTO. (2010). *AASHTO LRFD Bridge Design Specifications* (Fifth ed.). Washington, DC: American Association of State Highway and Transportation Officials.
3. WSDOT. (2010). *Bridge Design Manual (LRFD) M23-50.04*. Olympia, WA: Washington State Department of Transportation.
4. Haraldsson, O., Janes, T., Eberhard, M., and Stanton, J. (2013). *Precast Bent System for High Seismic Regions - Laboratory Tests of Column-to-Footing Socket Connections*, FHWA-HIF-13-039. Washington DC: Federal Highway Administration.
5. Hung, V., Stanton, J., and Eberhard, M. (2013). *Precast Bent System for High Seismic Regions - Laboratory Tests of Column-to-Drilled Shaft Socket Connections*, FHWA-HIF-13-038. Washington DC: Federal Highway Administration.
6. Mander, J., Priestley, M., and Park, R. (1988). Theoretical Stress-Strain Model for Confined Concrete. *Journal of Structural Engineering*, Vol. 114, No. 8. pp. 1804-1826.
7. Raynor, D. (2000). *Bond of Reinforcing Bars Grouted in Ducts*. Seattle, WA: Department of Civil and Environmental Engineering, University of Washington.
8. Pang, J., Steuck, K.P., Cohagen, L., Stanton, J., and Eberhard, M. (2008). *WA-RD 684.2 Rapidly Constructible Large-Bar Precast Bridge-Bent Seismic Connection*. Olympia, WA: Washington State Department of Transportation.